https://doi.org/10.5194/egusphere-2026-2338
Preprint. Discussion started: 28 April 2026

How precipitation lapse rates shape runoff simulations and flood frequency estimates in mountainous regions

Eleni Kritidou[1], Martina Kauzlaric[2], Maria Staudinger[1], Guillaume Evin[3], Marc Vis[1], Daniel Viviroli[1]

[1]Department of Geography, University of Zurich, Zurich, Switzerland
[2]Institute of Geography and Oeschger Centre for Climate Change Research, University of Bern, Bern, Switzerland
[3]Univ. Grenoble Alpes, CNRS, INRAE, IRD, Grenoble INP, IGE, Grenoble, France

Correspondence to: Eleni Kritidou (eleni.kritidou@uzh.ch)

Abstract. Precipitation lapse rates (PLRs) play a key role in hydrological simulations of mountainous catchments. However, they are often poorly represented in the precipitation estimates and are typically simplified as constant and positive values in the hydrological models. In this study, we combine a stochastic weather generator with a hydrological model to investigate how PLRs affect runoff simulations for several mountainous catchments in Switzerland. In the weather generator, the PLR adjusts precipitation from station elevation to mean catchment elevation, while in the hydrological model it redistributes precipitation among elevation zones. By systematically varying the PLRs in both the weather generator and the hydrological model between 0% and 10%, we found effects on mean seasonal and annual runoff, as well as on extreme floods, depending on catchment characteristics and precipitation network properties. Specifically, higher-elevation catchments were less sensitive compared to lower-elevation catchments. Increasing PLRs tended to increase summer floods, while decreasing PLRs tended to increase winter floods. In addition, the seasonality of frequent floods was more sensitive to changes in PLRs than that of rare floods. Moreover, flood seasonality was primarily controlled by the PLR in the hydrological model, while flood magnitude was mainly driven by the PLR in the weather generator through its effect on precipitation amounts. These findings highlight the need for a more comprehensive investigation of the assumption of a constant lapse rate in hydrological models, particularly in mountainous regions where precipitation gradients are strong and observations are limited.

1 Introduction

Precipitation lapse rates (PLRs) are often used to describe the variation of precipitation with elevation. They represent an empirical relationship that emerges from processes such as the uplift of humid air masses, which promotes convection and condensation. Thus, at aggregated time scales like season or year, precipitation generally increases with elevation, typically referred to as orographic enhancement (Barry and Chorley, 2010; Houze, 2012). However, at event scale this relationship is not evident as the spatial pattern of precipitation is influenced by the location where the precipitation event first occurs (Legrand et al., 2024). Additionally, this increase is not necessarily linear and may present a threshold effect at intermediate elevations (Avanzi et al., 2020; Napoli et al., 2019).

https://doi.org/10.5194/egusphere-2026-2338
Preprint. Discussion started: 28 April 2026

PLRs strongly influence the water balance of high-elevation catchments and, thus, also the seasonal dynamics of snow accumulation and melt, the snowpack distribution, and glacial mass balances (Bales et al., 2006; Bohne et al., 2020; Dettinger et al., 2004; Houze, 2012; Morán-Tejeda et al., 2013; Mott et al., 2014; Ragettli et al., 2014; Sarmadi et al., 2019; Sospedra-Alfonso et al., 2015; Viviroli et al., 2007). Short-duration orographic precipitation events in mountainous areas can be very intense and often trigger floods (Buzzi et al., 1998; Chen and Shi, 2023; Marra et al., 2021; Panziera et al., 2015) landslides, and avalanches Thus, PLRs play an important role in Earth's water budget (Jiang, 2003) and have utmost importance for water resources planning, agriculture, energy production, ecosystem conservation and natural hazard preparedness.

Despite this importance, the variation of precipitation with elevation remains poorly understood due to its highly localized nature, which depends on the synoptic weather state, the season, and the local topography (Bell et al., 2022; Benoit et al., 2024; Dura et al., 2024; Houze, 2012; Marra et al., 2021; Napoli et al., 2019; Ragettli et al., 2014; Ruelland, 2020; Sevruk, 1997). These complexities pose several challenges in operational hydrology. Additionally, estimating precipitation in mountainous regions is challenging due to the limited density of rain gauges at higher elevations (Frei and Schär, 1998; Guan et al., 2005; Masson and Frei, 2014; Roe, 2005; Ruelland, 2020; Shahgedanova et al., 2021; Suri and Azad, 2024; Wortmann et al., 2018). While Switzerland, for instance, has a comparatively dense gauge network most stations are located at low and intermediate elevations and higher elevations are underrepresented (Viviroli et al., 2011).

Different approaches have been proposed to address the precipitation variability arising from orographic enhancement and the resulting uncertainty in precipitation estimates in mountainous regions (Avanzi et al., 2020; Bertoncini and Pomeroy, 2025a; Medina and Houze, 2003). Various approaches to estimate PLRs rely on precipitation gauge observations and geostatistical techniques (Daly et al., 1994, 2008; Foehn et al., 2018; Frei and Schär, 1998; Isotta et al., 2019). Avanzi et al. (2020) derived a climatology of lapse rates combining snow-course data points with ground-based precipitation measurements. Orographic enhancement has also been studied with composite products, such as combining radar images with digital elevation models (Foresti and Pozdnoukhov, 2012) or combining radar or satellite data with rain gauge observations (Crochet, 2009; Foresti and Pozdnoukhov, 2012; Nie et al., 2015). Recently, Dura et al. (2024) evaluated seven different precipitation products (interpolation, reanalysis, satellite, radar, and regional climate model simulations) to determine their ability to capture the elevation dependence of annual and seasonal precipitation in France. They underlined that each product has its own uncertainties, such as underestimating precipitation at high elevations due to gauge undercatch. In that direction, Bertoncini and Pomeroy (2025) developed a framework for generating daily precipitation fields that account for the uncertainty in the elevation of the precipitation gauge network by explicitly varying lapse rates. The authors emphasize the importance of the uncertainty in mountain precipitation estimates due to lapse rates and suggest that resolving these inaccuracies would improve hydrological predictions of extreme events.

Hydrological catchment models are influenced by these uncertainties and may fail to close their water balance because they are sensitive to precipitation input amounts (Bardossy and Das, 2008; Bertoncini and Pomeroy, 2025a; Nicótina et al., 2008; Oudin et al., 2006). Uncertainties from precipitation inputs further propagate to runoff simulations. As discussed in detail in Ruelland (2020), further research is needed to determine best practices for generating precipitation inputs that lead to robust

https://doi.org/10.5194/egusphere-2026-2338
Preprint. Discussion started: 28 April 2026

streamflow simulations. Beyond that, assigning a realistic lapse rate a priori in hydrological models is difficult and typically involves assumptions and simplifications. Taken together, these factors make streamflow simulation in mountainous environments a challenging task (Ragettli et al., 2014; Ragettli and Pellicciotti, 2012; Verbunt et al., 2003), which highlights the need for a reliable representation of the underlying spatiotemporal processes of precipitation in these regions. That would lead to reliable estimates of high-intensity rainfall events that modelers would use for the estimation of natural hazards like flash floods.

In hydrological catchment models, PLRs are commonly used to account for the precipitation increase with elevation. Typically, observed precipitation is extrapolated from a gauging station or an average from several stations to the different elevation zones within a catchment. The importance of accurately representing these elevation gradients for robust hydrological modelling is increasingly recognized. For example, Immerzeel et al. (2014) emphasized that observed temperature and precipitation lapse rates are often highly variable and critically affect glacio-hydrological simulations. Simplified assumptions can lead to considerable errors in water balance estimations. According to Zhang et al. (2015) all runoff components, including snowmelt, glacier melt and rainfall runoff, are sensitive to both temperature and precipitation lapse rates. For a Tibetan catchment, the authors demonstrated that accurately estimating these lapse rates could considerably improve snowmelt simulations. Similarly, Kumar et al. (2022) concluded that incorporating and calibrating elevation-dependent temperature and precipitation lapse rates in a hydrological model markedly improved water balance and streamflow simulations compared to omitting them or not calibrating them for a Himalayan river basin. Sensitivity analyses have also highlighted how the choice of PLR influences model simulations. Turpin et al. (2000) reported that simultaneously modifying the precipitation lapse rate (5% and 10%) and the upper limit above which precipitation increases with a different rate (800 m, 1400m, 1700m) can improve both snowpack and runoff simulation in the hydrological model HBV. They found that reducing the lapse rate to 5 % per 100 m and raising the upper limit elevation to 1700 m produced the most accurate simulations of snow-covered area while preserving or slightly improving runoff simulation performance. Some researchers have computed precipitation lapse rates from observational data for a given region and applied a constant value within the hydrological model (Gafurov et al., 2006; Zelelew and Alfredsen, 2013; Zhang et al., 2015), while others have used constant lapse rates that vary across certain elevation zones (Hegdahl et al., 2021; Ren et al., 2018).

In most hydrological modelling setups, a constant, observed or empirical precipitation lapse rate is assigned a priori (Kobold and Brilly, 2006; Akhtar et al., 2009; Driessen, 2010; Geris et al., 2015; Pool et al., 2017, 2018; Girons Lopez et al., 2020a; Al-Safi and Sarukkalige, 2020; Esmaeili-Gisavandani et al., 2021; Pool et al., 2021; Budhathoki et al., 2023; Clerc-Schwarzenbach et al., 2024, 2025). Even in large sample studies where catchments with considerably different physiographic characteristics are studied, a constant lapse rate is often prescribed (Clerc-Schwarzenbach et al., 2024; Clerc-Schwarzenbach and Do Nascimento, 2026; Hegdahl et al., 2021; Parajka et al., 2005). Thus, the relationship between mean daily precipitation and elevation is assumed to be linear and positive, and the impact of this modelling decision is overlooked.

Based on the above, we here investigated how precipitation lapse rates influence runoff simulations and particularly floods in selected catchments with a complex topography, focusing on Switzerland with its prominently mountainous terrain including

https://doi.org/10.5194/egusphere-2026-2338
Preprint. Discussion started: 28 April 2026

the Alps and the Jura Mountains. To do so, we used a model chain with long, synthetic time series from a stochastic weather generator (GWEX) and a hydrological catchment model (HBV). Both model chain components involve a lapse rate. In the weather generator, the lapse rate is employed to adjust precipitation from station elevation to mean catchment elevation, while in the hydrological model the lapse rate is used to redistribute the mean areal precipitation inputs to the different elevation zones. We performed simulations by varying the lapse rates consistently in both components from 0% to 10%. Because the results of these simulations reflect the combined effect of both lapse rates, we further aim to isolate the sensitivity attributed solely to the lapse rate within the hydrological model by varying it between 0% and 10% while keeping the precipitation input fixed. This allows us to clarify its role, which is often overlooked in hydrological studies in mountainous regions. Thus, our primary objectives were:

- To evaluate the sensitivity of flood estimates to variations of PLRs when applied in both precipitation interpolation and the hydrological model.
- To evaluate the sensitivity of flood estimates to variations in the PLR parameter applied exclusively within the hydrological model.

2 Study catchments and observational data

2.1 Study catchments

Simulations were performed for 27 Swiss catchments with different properties and flood regimes without major human alteration of runoff (Fig. 1). The size of the selected catchments varied between 21 km^2 and 1702 km^2, with mean elevations ranging from 596 m a.s.l. to 2,469 m a.s.l. The catchments belong to four large river basins that cover part of the Plateau, the pre-Alps, the Alps and the Southern Alps (Fig. 1) and all represent typical mountainous catchments.

2.2 Observational data

For this study, we derived meteorological and hydrological data from observational networks. Precipitation and temperature observations were available for 120 and 34 stations respectively at a daily scale for 1930–2019. These daily observations were supplemented by hourly data from 1990–2019.

For each study catchment, hourly discharge observations were provided by the Federal Office for the Environment (FOEN). This dataset was used for hydrological model calibration and evaluation and spans from 6 to 96 years within the period 1923–2019, with a median record length of 45 years.

https://doi.org/10.5194/egusphere-2026-2338
Preprint. Discussion started: 28 April 2026

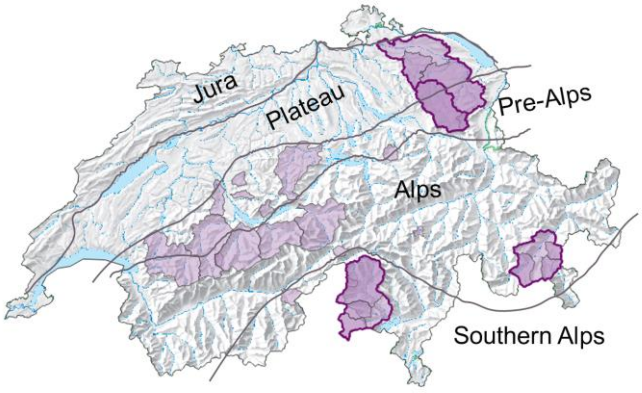

Figure 1 Map of Switzerland with study catchments. The dark purple colour shows the catchments that were also fully modeled with HBV and their sub-catchments. Relief map: Swiss Federal Office of Topography.

3 Methodology

3.1 Simulation workflow

Our approach is based on a modelling chain with long continuous simulations (CS). A multi-site stochastic weather generator (GWEX) (Evin et al., 2018, 2019) was parameterized based on the observational records and then used to produce 30,000 years of synthetic precipitation and temperature time series at an hourly time step. In GWEX, the lapse rate is used to adjust precipitation for the elevation difference between stations and the mean catchment elevation prior to spatial interpolation to mean areal precipitation using Thiessen weights. We did this adjustment using 5 different lapse rates (PLR_WG: 0%, 2.5%, 5%, 7.5%, 10% per 100m). That leads to five different MAP synthetic time series which serve as inputs to the bucket-type hydrological model HBV.

HBV includes a precipitation lapse rate parameter that redistributes the precipitation amount across the catchment's elevation zones (PLR_HBV). For any subsequent changes to the lapse rate value employed in the weather generator (PLR_WG), the same value was also used in the hydrological model (PLR_HBV) (see Fig. 2).

The results of these simulations include the combined effect of PLR_WG and PLR_HBV as they were altered simultaneously. To explore the contribution of the internal lapse PLR_HBV, we performed a one-at-a-time sensitivity analysis**.** We used the MAP inputs adjusted with a 5% PLR_WG to perform simulations while varying only the internal lapse rate to 0%, 2.5%, 5%, 7.5% and 10%. We do so because the combination of PLR_WG and PLR_HBV as 5% has been previously used for flood risk assessment (Kritidou et al., 2025, 2026; Staudinger et al., 2025; Viviroli et al., 2022) and serves as a baseline for comparison. Additionally, for the model calibration, PLR_WG and PLR_HBV were both set to 5%. For this experimental set-up, all other calibrated parameters remain the same and are derived from the 5% lapse rate. For all combinations of lapse rates, the annual maximum floods (AMFs) were extracted from the corresponding simulations, and a flood frequency analysis was performed.

https://doi.org/10.5194/egusphere-2026-2338
Preprint. Discussion started: 28 April 2026

3.2 Weather generator

GWEX was used to generate long time series of precipitation and temperature, which served as inputs for HBV. GWEX is a multi-site, two-part stochastic weather generator (Evin et al., 2018) designed to reproduce the most important characteristics of precipitation at different spatial and temporal scales and focusing on extremes. For this reason, it has been used in previous studies for flood risk assessments (Kritidou et al., 2026; Staudinger et al., 2025; Viviroli et al., 2022).

As a first step, GWEX is parameterized based on the daily weather observations (1930–2019) and relies on a two-state Markov chain (Wilks, 1998) to model the precipitation occurrence at a single site (station). The spatial structure (inter-site correlations) is modelled with an unobserved Gaussian process. The Extended Generalized Pareto Type III Distribution (EGPD) (Naveau et al., 2016) is used to generate the daily precipitation intensities at each site. The distribution provides a smooth transition between a gamma-like distribution and a heavy-tailed Generalized Pareto Distribution (GPD). This feature makes EGPD suitable to describe the upper tail behaviour of precipitation, associated with high rainfall intensities. A set of parameters is estimated for each month based on a 3-month window to account for the seasonality of precipitation characteristics, resulting in 12 parameter sets. Further details about GWEX properties can be found in Evin et al. (2019, 2018).

The daily amounts generated with GWEX are then disaggregated to hourly values using the method of analogues on basis of hourly observations from 1990 to 2019 (see details in Evin et al., 2019, 2018; Kritidou et al., 2025; Staudinger et al., 2025; Viviroli et al., 2022). Analog days are selected within the same intensity and seasonality classes by comparing the daily precipitation field of each simulated day with that of 1990–2019. The best analogue day is then selected from a pool of 100 analogues that are retained based on a distance criterion.

Overall, GWEX generated 30,000 years of long time series (i.e., 30 scenarios of 1,000 years each) for each station on an hourly time scale. Precipitation at each station is individually treated with a lapse rate (PLR_WG) to adjust the data from station elevation to mean catchment elevation. Then, the adjusted precipitation station data are interpolated with Thiessen weights to determine mean areal precipitation (MAP). Here, we vary PLR_WG in a reasonable range (0%–10%) to explore its impact on runoff simulation.

3.3 Hydrological model

For the simulations, we used the hydrological catchment model HBV (Bergström, 1992; Seibert and Bergström, 2022) in the version HBV-light (Bergström, 1992; Seibert and Bergström, 2022; Seibert and Vis, 2012). HBV is a bucket-type model with four main routines: (i) snow, (ii) soil moisture, (iii) response (or groundwater), and (iv) routing. For catchments with a glacier cover of 1% or more, a glacier routine is included. The snow, soil and glacier routine are computed for each elevation and zone. For the simulations, a fixed MAP and a mean areal temperature were used as given by the weather generator. We used a warm-up period of 10 years. Table 1 shows the calibrated and fixed parameters (Staudinger et al., 2025; Viviroli et al., 2022) for each routine.

https://doi.org/10.5194/egusphere-2026-2338
Preprint. Discussion started: 28 April 2026

Table 1 Parameters of the HBV hydrological model. gw: groundwater.

https://doi.org/10.5194/egusphere-2026-2338
Preprint. Discussion started: 28 April 2026

Parameter	*Routine*	*Description*	*Unit*	*Range*
TT	Snow	Threshold temperature	[°C]	-2.5 – 2.5
CFMAX	Snow	degree-day factor	[mm/(h°C)]	0.001 – 5
SFCF	Snow	snow correction factor	[–]	0.4 – 1.6
CFR	Snow	Refreezing coefficient	[–]	0.05 (fixed)
CWH	Snow	Snow water holding capacity	[–]	0.1 (fixed)
FC	Soil	Maximum storage in soil box	[mm]	50 – 1000
LP	Soil	Threshold reduction	[–]	0.3 – 1
BETA	Soil	Shape coefficient	[–]	1 – 5
PERC	Soil	Max flow from upper to lower gw bucket	[mm/h]	0 – 1
Alpha	Response	Shape coefficient	[–]	0 – 1
K1	Response	Recession coefficient (upper gw bucket)	$[h^{-1}]$	0.0001 – 0.1
K2	Response	Recession coefficient (lower gw bucket)	$[h^{-1}]$	0.00001 – 0.05
MAXBAS	Routing	Factor of triangular weighting	[h]	1 – 100
KGmin	Glacier	Minimum outflow coefficient	$[h^{-1}]$	0.0001 – 0.2
CFGlacier	Glacier	Correction factor glacier	[–]	1 – 2
KSI	Glacier	snow-to-ice conversion factor	$[h^{-1}]$	$5 \cdot 10^{-5}$
RangeKG	Glacier	Max minus min outflow coefficient	$[h^{-1}]$	0 (fixed)
CFSlope	Glacier	Correction factor slope	[–]	1 (fixed)

https://doi.org/10.5194/egusphere-2026-2338
Preprint. Discussion started: 28 April 2026

PCALT	Catchment	Precipitation lapse rate	[%/100m]	0, 2.5, 5, 7.5, 10
TCALT	Catchment	Temperature lapse rate	[°C/100m]	Time series (see below)

The model was calibrated for the 27 study catchments with the 5% PLR_WG and PLR_HBV using a genetic algorithm (Seibert, 2000), and the Nash-Sutcliffe efficiency (Nash and Sutcliffe, 1970) as objective function. To account for parameter uncertainty, each catchment was calibrated independently 100 times against observed discharge resulting in an ensemble of 100 suitable parameter sets. However, due to the high computational cost of running simulations with long synthetic time series, we selected three representative parameter sets. These represent the lower, median, and higher range of flood responses, selected using a percentile-based approach (see Sikorska-Senoner et al., 2020 for details). Here, we present results based on the median parameter set for all PLR_WG and PLR_HBV.

In the HBV model, the precipitation lapse rate is a model parameter, PCALT (%/100m), which redistributes precipitation to the different elevation zones, without altering the total precipitation amount. For our experimental setup, we altered only PCALT and kept all other parameters at the values obtained from calibrating the model using a 5% precipitation lapse rate. Recalibrating the model for each PCALT value would lead to compensation effects and is beyond the scope of this study. For temperature, we always used a specific lapse rate (TCALT [°C/100 m]) for each calendar day, computed from temperature observations.

For our application, the snow routine is particularly important because it can compensate for systematic errors in the snowfall measurements and for the `missing' evaporation from the snowpack in the model. The extent of this compensation depends on the hypsography of a catchment (Staudinger et al., 2025). The threshold temperature is critical because it defines whether precipitation is simulated as snow or rain. When the air temperature is below the threshold temperature, precipitation is classified as snow and multiplied by a snowfall correction factor, SFCF [-]. Thus, we calculate the elevation h at which phase portioning occurs, i.e., the transition from rain to snow or vice versa, with

$$h = h_0 \frac{100(T_0 - T_T)}{T_{CALT}} \quad (1)$$

where h_0 is the mean catchment elevation, T_0 is the temperature at mean catchment elevation, T_T is the threshold temperature, and T_{CALT} is the temperature lapse rate.

3.4 Flood frequency analysis

Hydrological simulations were performed for all combinations of lapse rates mentioned in section 3.1. In total, we performed 9 runs: 5 where PLR_WG and PLR_HBV were identical and another 4 where only PLR_HBV was varied and PLR_WG was kept at 5%. Then, for each scenario of 1000 years we extracted AMFs and assigned a return period. That led to 30 estimates per return period up to 1000 years, which allows us to comprehensively compare flood estimates in terms of their

https://doi.org/10.5194/egusphere-2026-2338
Preprint. Discussion started: 28 April 2026

seasonality and magnitude as well as their corresponding dispersion. The combination of PLR_WG = PLR_HBV = 5% serves as a basis for comparison against the other PLRs (0%, 2.5%, 7.5%, 10%).

3.5 Indicators for the influence of PLRs

For our analysis, we used various indicators to compare our results and to understand the influence of the precipitation lapse rate. First, we used the flood seasonality ratio $R_{F,}$ which is defined as

$$R_f = \frac{Q_{95(\text{summer})}}{Q_{95(\text{winter})}} \quad 2$$

where $Q_{95(summer)}$ represents the 95th percentile of the summer AMFs (April–September) and $Q_{95(winter)}$ the 95th percentile of the winter AMFs (October–March). For R_F>1, summer floods are more severe than winter floods, and for R_F<1 winter floods more severe than summer floods. Thus, by assessing how R_F is changing (ΔR_F) with PLR, we better understand if the catchments shift more to summer or winter floods.

Second, we employed the confidence interval amplitude (CIA) (Equation 3) to assess the impact of PLR on the spread of simulated extremes. It is a normalized measure of uncertainty that has been used in previous studies (Arnaud et al., 2017; Kritidou et al., 2025) and is defined as

$$CIA = \frac{Q_{95} - Q_5}{Q_{50}} \quad 3$$

where Q_{95}, Q_5 and Q_{50}represent the 95th, 5th and 50th percentile of discharge, respectively.

Third, we used a redistribution index to quantify the impact of precipitation redistribution across elevation zones within the catchment as

$$RI = \sum_{i=1}^{n} \left[\frac{A_i}{A} \cdot |E_i - E_{mean}| \right] \quad 4$$

where A_i is the area of the elevation zone i, A is the catchment area, E_i is the elevation of the elevation zone i and E_{mean} is the mean catchment elevation.

Fourth, we calculate the sensitivity coefficient (elasticity) of runoff components to changes in precipitation resulting from variations in the precipitation lapse rate in GWEX (PLR_WG). This concept has been widely applied in hydrometeorological studies (Andréassian et al., 2016; He et al., 2025; Zhang et al., 2022) as it can evaluate the sensitivity of streamflow to changes in other climate variables, usually relative to the long-term mean of time series (Schaake, 1990). It has been widely used on annual and aggregated timescales (see Zhang et al. (2022)) for multi-annual timescales). Here, we focus on different runoff components on seasonal timescales. Thus, the sensitivity is given by:

https://doi.org/10.5194/egusphere-2026-2338
Preprint. Discussion started: 28 April 2026

$$\varepsilon = \frac{\frac{dQ}{\bar{Q}}}{\frac{dP}{\bar{P}}} \quad (5)$$

where ε is the sensitivity coefficient of runoff Q to precipitation P, indicating that a 1 % change in P leads to an ε% change in Q. $\bar{P}, \bar{Q}$ are the multi-year average precipitation and simulated runoff, respectively, both based on the baseline (PLR 5%). The operator d represents the difference between seasonal and average values. Therefore, ε is calculated as the slope of a linear regression line fitted to the seasonal data. It should be noted that, the multi-year average of the 5% lapse rate is used as the reference, as we are interested in assessing the percentage changes of streamflow resulting from the percentage changes in precipitation.

Lastly, we introduce the coefficient of variation to quantify the variability in the frequency of occurrence of floods simulated with different lapse rates. To do so, we use the 30 AMFs corresponding to each return period and estimate their seasonality. For each PLR, we count how many of the events with the same return period occur in each month. Then, we calculate the coefficient of variation based on the number of occurrences across months, lapse rates and return periods. For a specific month (m) and return period (RP), the coefficient of variation is defined as

$$CV_{m,RP} = \frac{\sigma_{m,RP}}{\mu_{m,RP}} \quad (6)$$

where m is the month of the year, σ is the standard deviation of the number of events frequency events in month m across the five PLRs, for a given return period and μ is the corresponding mean. Thus, the larger the CV, the larger the shift in the month of occurrence of the floods among the PLRs. Ultimately, for each catchment and RP we calculate the mean coefficient of variation, as the mean $CV_{m,RP}$ across all months with at least one event.

https://doi.org/10.5194/egusphere-2026-2338
Preprint. Discussion started: 28 April 2026

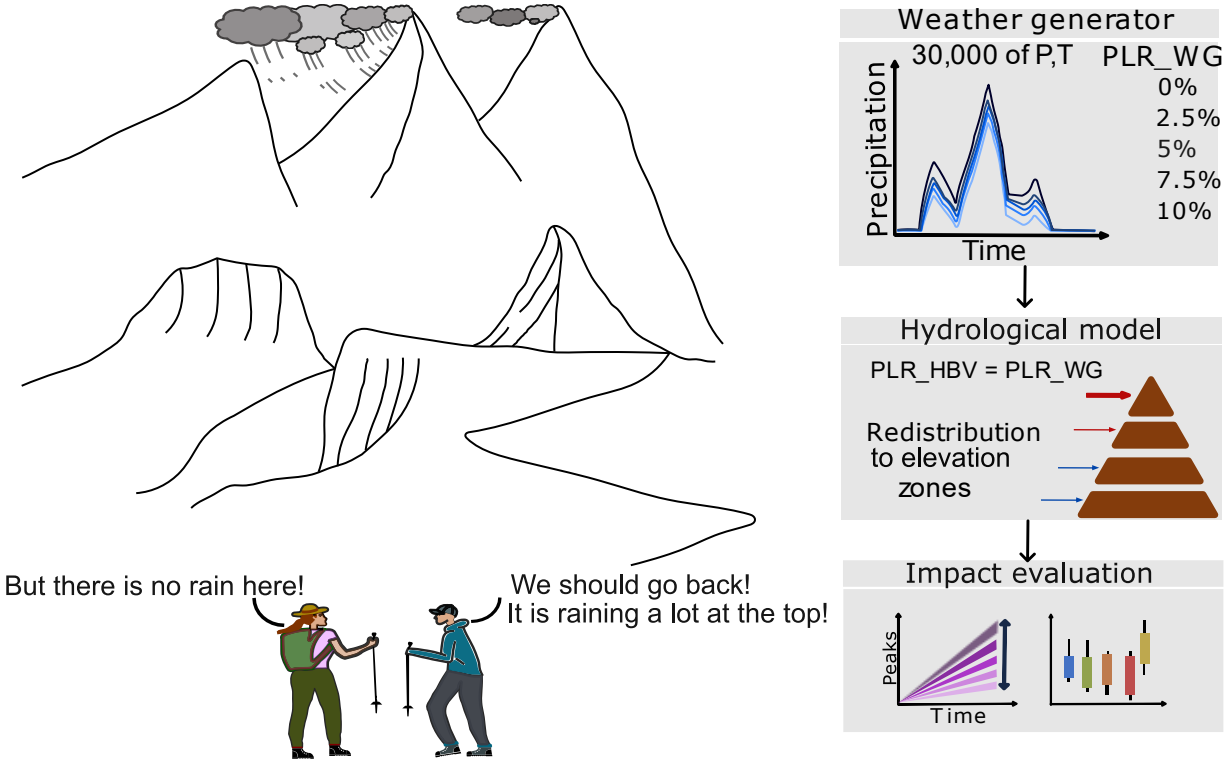

Figure 2 Schematic representation of the methodological steps. P and T are precipitation and temperature, respectively. PLR_WG and PLR_HBV are the precipitation lapse rates employed in the weather generator and the hydrological model, respectively.

4 Results

4.1 Precipitation properties

As a first step in the analysis, we calculated the number of stations at different elevation bands and the mean length of the observations based on the stations considered for each catchment. We also calculated the difference between the mean catchment elevation and the mean station elevation (ΔElevation), using Thiessen weights. The stations cover well elevation ranges between 500 and 1500 m a.s.l., whereas station density is sparse at higher regions (see Fig. 3b and Table 2). The relationship between differences in mean annual precipitation from the weather generator (computed with PLR_WG = 0%, 2.5%, 7.5%, and 10% relative to the baseline 5%) and ΔElevation is illustrated in Fig. 3b for all catchments. Relative changes are positive for PLRs above 5% and negative for those below 5%. Changes in mean annual precipitation show a clear linear correlation with ΔElevation: catchments with a greater discrepancy between mean catchment elevation and mean station elevation show larger changes in annual precipitation, reaching values of up to ±40%.

Generally, higher mean catchment elevations corresponded to larger discrepancies between mean station elevation and mean catchment elevation (Pearson's r = 0.59 for the linear correlation, $p<0.05$). This relationship was affected by both the density

https://doi.org/10.5194/egusphere-2026-2338
Preprint. Discussion started: 28 April 2026

of the network and the mean length of the observations. Catchments with smaller discrepancies between mean station elevation and mean catchment elevation tend to show longer mean record lengths (green points), while the opposite is true for catchments with larger discrepancies (light green and yellow points). In some cases, however, ΔElevation remains relatively small for catchments with a mean elevation of more than 2000 m a.s.l. because they are still well represented by stations or because only a few high-elevation stations are considered for small catchments.

Table 2 Number of precipitation gauging stations per elevation band based on all catchments

Number of stations	*Elevation range [m a.s.l.]*
15	<500
39	500–1000
30	1000–1500
12	1500–2000
6	>2000

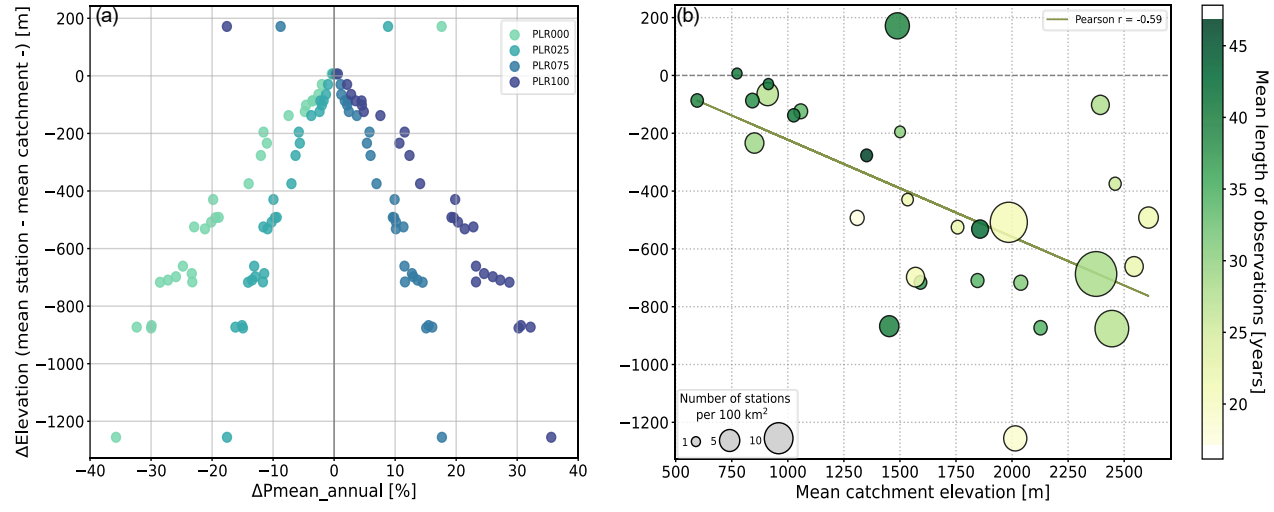

Figure 3 Relationship between elevation discrepancy (difference between mean catchment elevation and mean Thiessen-weighted station elevation), drawn against (a) the relative differences in mean annual precipitation of the baseline (5% lapse rate in GWEX) and the other four lapse rates examined (0%, 2.5%, 7.5% and 10%) and (b) mean catchment elevation of the corresponding catchment. The size indicates the number of stations per catchment and the colour the mean length of the observations from these stations

4.2 Threshold elevation

Precipitation and temperature lapse rates are crucial parameters because they influence both the amount and the form (rain or snow) of precipitation at different elevations within a catchment. Although, in reality, the rain snow partitioning depends in various atmospheric and topographic factors, in the HBV model, this is done by multiplying precipitation with the SFCF

https://doi.org/10.5194/egusphere-2026-2338
Preprint. Discussion started: 28 April 2026

parameter depending on the threshold temperature parameter (Table 1). We calculated the elevation above which precipitation falls as snow based on Equation 1 on a monthly scale (see Fig. 4 for two exemplary catchments, the Sarine and the Maggia). We call this threshold elevation. Note that negative threshold elevations are possible, indicating that the threshold elevation is very low (i.e., below sea level) and that snowfall occurs across the entire catchment.

The threshold elevation is higher in summer and lower in winter, depending on air temperature. In January, for example, precipitation will on average be simulated as snow above an elevation of 800 m a.s.l. for the Sarine catchment and above nearly 1000 m a.s.l. for the Maggia catchment. In July, when temperatures are higher, snowfall occurs only above 3500 m a.s.l. in both catchments (Fig. 4).

We further estimated the area below the threshold elevation (Fig 4c), which represents the percentage of the catchment where precipitation is simulated as rain. Values above 50% indicate that the threshold elevation exceeds the mean catchment elevation and that precipitation is predominantly simulated as rain in most catchment elevation zones. Conversely, values below 50% indicate that precipitation is simulated as snow in most elevation zones. Fig. 4c shows the monthly pattern of the area below threshold elevation across all catchments. The smallest percentages occur during winter months, with most of the catchments showing almost no area below the threshold elevation. In these cases, even lower elevation zones will receive snow. However, snow at low elevations is usually wet. When the 0% lapse rate is applied (no redistribution of precipitation across elevations and therefore, in comparison to larger lapse rates, more precipitation in lower elevation zones) this leads to more direct snowmelt rather than snow accumulation and snowpack development during the winter season. During summer, the area below threshold elevation is zero for nearly all catchments, and thus precipitation is simulated as rain for almost the entire catchment. Lastly, a mixed pattern is observed in March, April and November, indicating that temperature rise and fall in combination with catchment elevation play a critical role in determining whether a given catchment receives predominantly snow or rain.

https://doi.org/10.5194/egusphere-2026-2338
Preprint. Discussion started: 28 April 2026

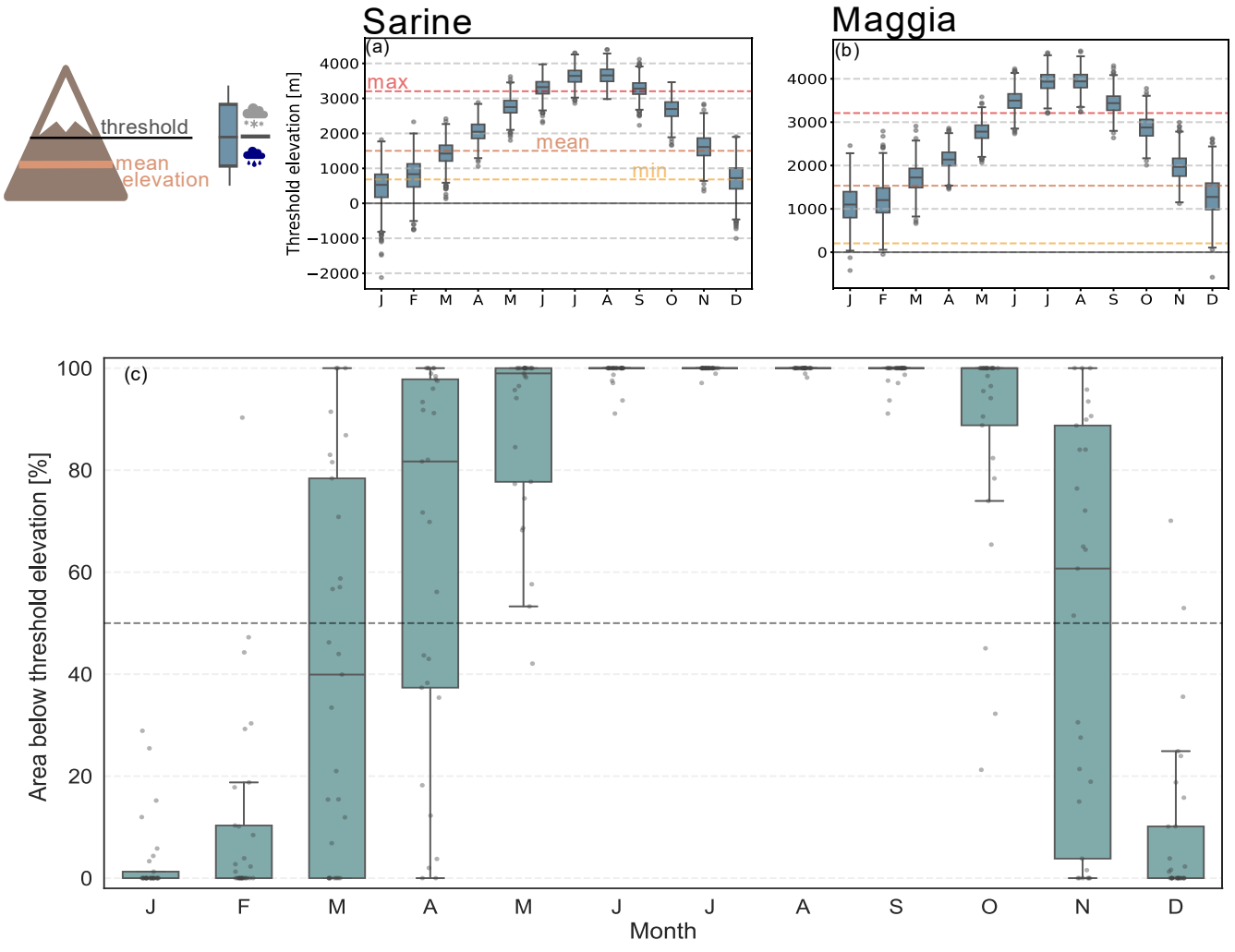

Figure 4 Monthly variation of the threshold elevation for two example catchments: (a) the Sarine and (b) the Maggia. The red dashed line indicates the maximum catchment elevation zone, while the orange and yellow lines indicate the mean and minimum elevation zones, respectively. For illustration purposes, one realization of 1000 years is shown. Thus, each boxplot s based on 1000 values (one per year) representing the monthly threshold elevation. Panel (c) shows the monthly variation in the percentage of the catchment area that is below the threshold elevation. The area below the threshold elevation has been calculated based on the mean threshold elevation over all 30 scenarios (see panels a and b for one scenario). Each point represents one catchment.

4.3 Impact on runoff components

To understand how sensitive catchments and runoff components are to changes in lapse rates in both the weather generator and the hydrological model, we computed the sensitivity of different runoff components to precipitation changes induced by varying lapse rates for different seasons. Fig. 5 shows how these sensitivity coefficients vary with elevation. The change in precipitation and runoff was estimated relative to the baseline runs, defined by a PLR of 5% both in the weather generator and the hydrological model. For total simulated runoff (Q_total; left panels), sensitivity is positive during all seasons, indicating

https://doi.org/10.5194/egusphere-2026-2338
Preprint. Discussion started: 28 April 2026

that increasing the PLRs leads to higher total runoff, whereas decreasing the PLRs leads to lower total runoff for most catchments (Fig. 6). Additionally, sensitivity was found to be negatively correlated to mean catchment elevation, indicating that lower-elevation catchments are more sensitive to changes in precipitation.

Notably, precipitation has the strongest impact on total runoff in summer, with sensitivity coefficients ranging from 0.4 to almost 2. This indicates that, depending on the catchment, a 10% change in precipitation results in a 4–20% change in total runoff. Specifically, the sensitivity of rainfall runoff shows a stronger correlation with elevation than snowmelt and glacier runoff during the summer season. This correlation is very similar for all PLRs. Furthermore, the sensitivity coefficients of snowmelt do not differ significantly among PLRs, but they vary depending on the season and elevation. While small but positive sensitivity coefficients occur in winter and spring, they are close to zero in summer for almost all catchments. That suggests that precipitation change does not drive summer snowmelt. In autumn, more pronounced sensitivity coefficients (values above 1) are noted in lower elevation catchments, and they gradually decrease with increasing elevation. Hence, changes in PLRs are the dominant factor controlling changes in snowmelt runoff for lower-elevation catchments. The glacier melt runoff sensitivity coefficients were negative for almost all catchments and seasons, indicating that an increase in precipitation leads to a decrease in glacier melt runoff, whereas a decrease in precipitation leads to an increase in glacier melt runoff. Although the correlation with elevation is stronger in winter and spring, the results show an inverse correlation between small (<5%) and large PLRs (>5%). However, it is difficult to interpret the relationship between sensitivity coefficient and elevation, as the number of data points available is limited and the correlation is statistically not significant.

https://doi.org/10.5194/egusphere-2026-2338
Preprint. Discussion started: 28 April 2026

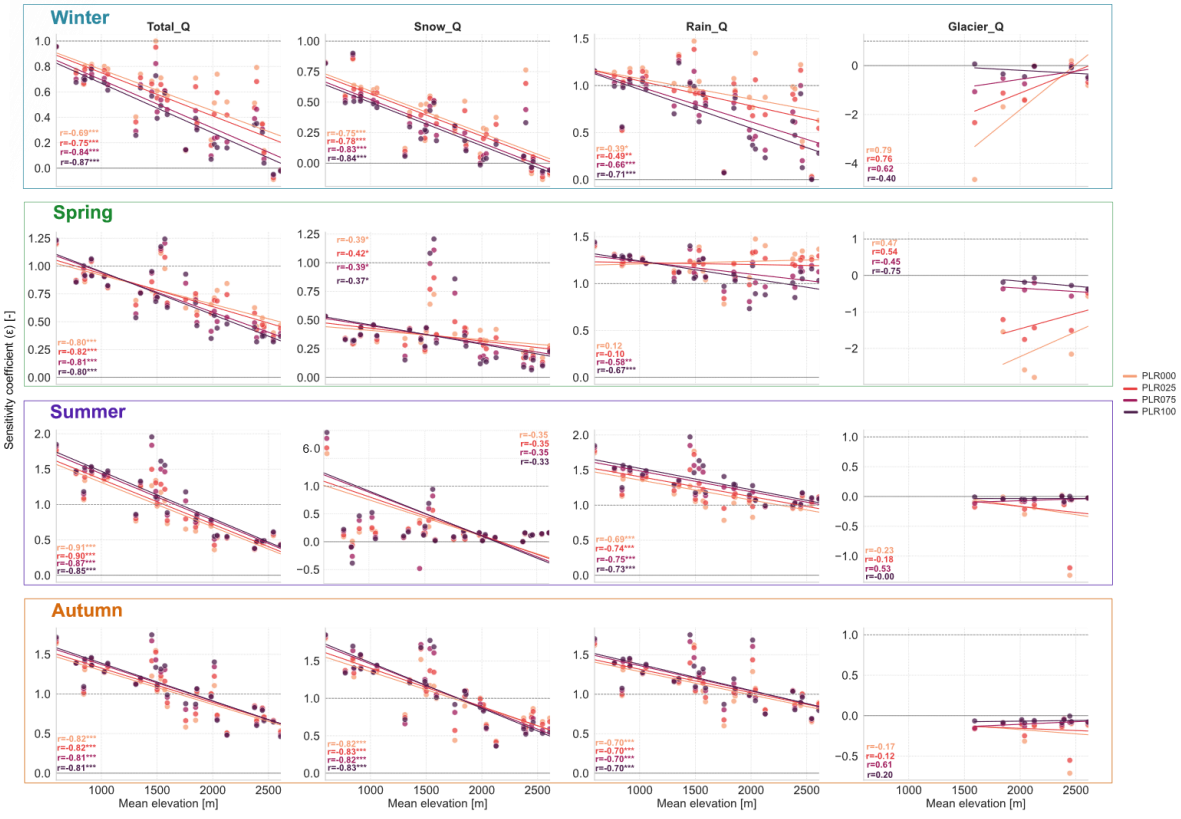

Figure 5 Sensitivity coefficient of total runoff, snowmelt runoff, rainfall runoff and glacier runoff in response to precipitation changes induced by varying PLRs, plotted against elevation for winter, spring, summer, and autumn. The sensitivity coefficients are calculated relative to the baseline, with a lapse rate of 5% for both GWEX and HBV. Each point represents one catchment.

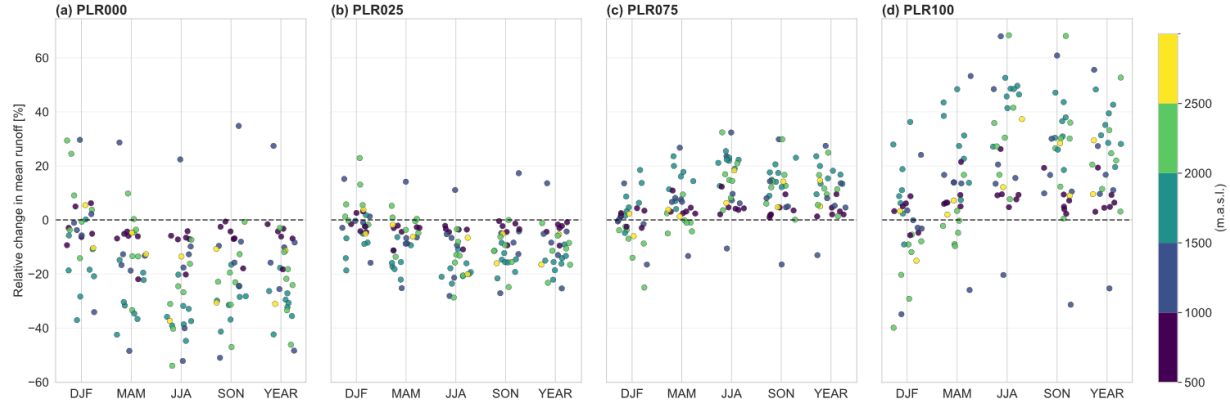

340

Figure 6 Changes in mean seasonal and annual runoff simulated under different PLRs relative to the baseline, with a lapse rate of 5% for both GWEX and HBV. Colours indicate the mean elevation of the study catchments.

https://doi.org/10.5194/egusphere-2026-2338
Preprint. Discussion started: 28 April 2026

4.4 Impact on seasonality and magnitude of extremes

Fig. 7 shows the percentage of flood events occurring per month (panels a and c) and their mean magnitude (panels b and d) for two example catchments. The percentages are calculated based on all 30,000 AMFs. As the PLRs decrease, the frequency of floods declines during summer and increases during winter and early spring (see also the mean flood date in Fig. S1). For almost all catchments, winter floods are predominant with the 0% PLR (green line in panels a, c). During winter and early spring (Dec–Apr), lower PLRs result in a higher percentage of flood events. Conversely, the frequency of events during the summer months is positively associated with higher PLRs. Regarding flood magnitude, there is a consistent positive relationship: higher PLRs result in larger mean AMFs throughout the entire year. Consequently, the largest floods occur when PLRs are highest (10%) and gradually decrease with the decrease of PLRs.

To further understand this change in flood seasonality, we calculated the flood seasonality ratio (R_F) from the AMFs simulated with all PLRs and then estimated the relative change (ΔR_F) between the 5% (baseline) and the other PLRs. The majority of the catchments shifted towards summer floods ($\Delta R_F > 0$) as annual maximum precipitation increases, and towards more severe winter floods when annual maximum precipitation decreases (Fig. 7e). Specifically, we observed a positive correlation (r = 0.40) between changes in mean annual maximum precipitation and the flood seasonality ratio R_F (both calculated relative to the 5% PLRs). Smaller changes in the mean annual maximum precipitation and R_F mostly occur in catchments with smaller ΔElevation (yellow points). This indicates that catchments with high ΔElevation tend to shift more towards winter or summer floods (darker points) when the lapse rate increases or decreases.

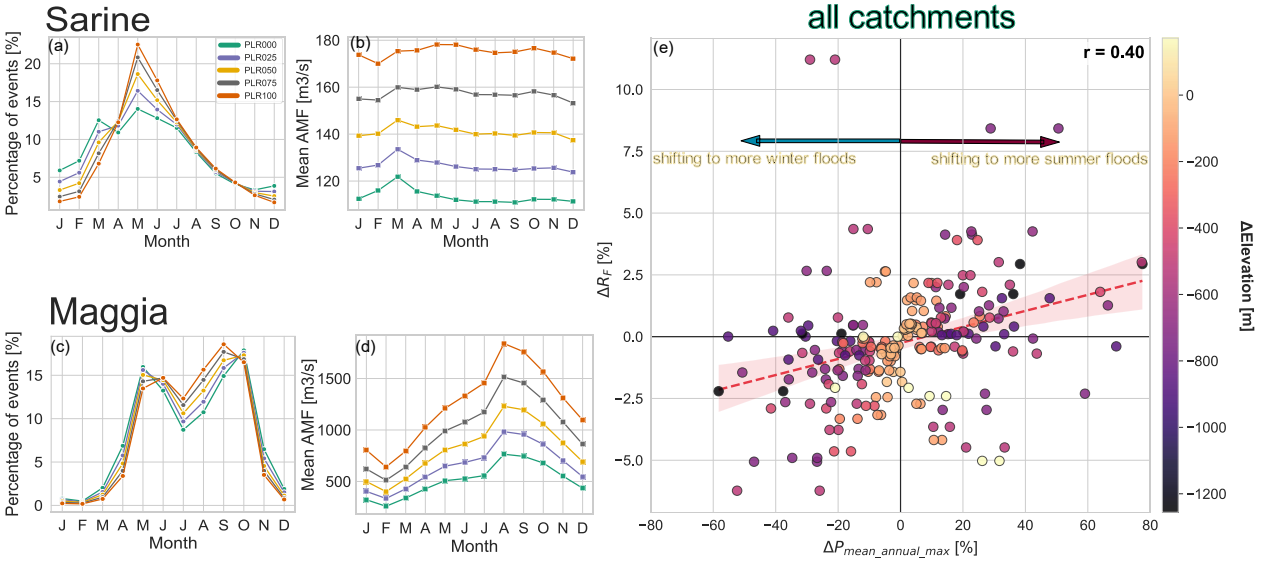

Figure 7 Percentage of AMFs per month simulated with varying PLRs for the (a) Sarine and (b) Maggia catchments, and the corresponding mean magnitudes in panels (b) and (d) respectively. Panel (e) shows the relationship between the change in the flood seasonality ratio and the change in mean annual precipitation relative to the baseline. Each catchment is represented by four points, corresponding to relative changes from the baseline to the 0%, 2.5%, 7.5% and 10% PLRs. Point colours represent ΔElevation.

https://doi.org/10.5194/egusphere-2026-2338
Preprint. Discussion started: 28 April 2026

To further understand the effect of PLRs on flood generation mechanisms, we calculated the mean coefficient of variation (CV) of flood seasonality per return period. First, the CV was calculated for each catchment based on the number of events per month, return period, and lapse rate. These 12 coefficients were then used to calculate the mean CV per catchment (Fig. 8). The boxplots illustrate a decrease in CV with return period, underscoring that the month in which frequent floods occur is highly variable in response to changes in PLRs, whereas variability decreases for larger return periods. This low variability in the seasonality of large floods – in combination with the finding that large floods occur in the summer season (Fig 7) – suggests that the large rainfall-driven events dominate during summer regardless of the chosen PLRs. Consequently, more frequent floods appear to be more sensitive to the changes in PLRs, whereas the mechanisms generating large floods appear to be less affected.

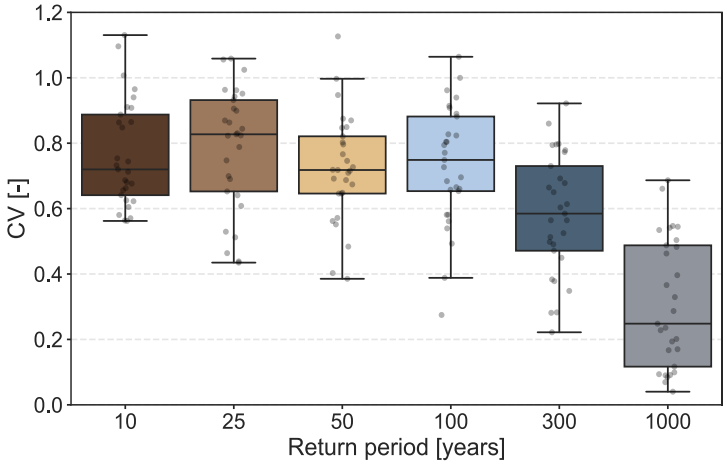

Figure 8 Mean coefficient of variation of the seasonality of flood events for different return periods (10, 25, 50, 100, 300, and 1000 years).

4.5 Snow contribution

The monthly variation in the contribution of snowmelt to simulated flood peaks varies across months and catchments when varying both PLRs (Fig. 9). We found that the model's lapse rate is mainly responsible for the clear change in the seasonal pattern of snowmelt contribution because we achieved similar results when only PLR_HBV was varied. From November to February, the contribution of snowmelt to total runoff is inversely correlated to PLRs, with smaller PLR values leading to larger snowmelt contributions. In March and April, all PLRs show nearly identical snowmelt contributions. From May to September, the contribution of snowmelt becomes positively correlated with PLRs but gradually decreases.

The inverse correlation observed during winter (November to February), where smaller PLRs lead to larger snowmelt contributions, is attributed to the spatial distribution of precipitation and snow accumulation. When small PLRs (e.g., 0% or 2.5%) are applied, precipitation increases at lower elevations, and snow accumulation decreases at high elevations compared

https://doi.org/10.5194/egusphere-2026-2338
Preprint. Discussion started: 28 April 2026

to the higher PLRs. Snow at lower elevations, below the threshold elevation, is wet (Blanchet et al., 2009) and leads to snowmelt. This effect is apparent because in winter, a larger portion of the catchment receives snowfall (Fig. 4).

In contrast, during late summer and early fall, when the threshold elevation moves to higher elevations (Fig. 4), snow contributes minimally to floods. The PLRs still are positively correlated with the snowmelt contribution, but the changes in mean values are small. Consequently, flood generation is dominated by high rainfall intensities.

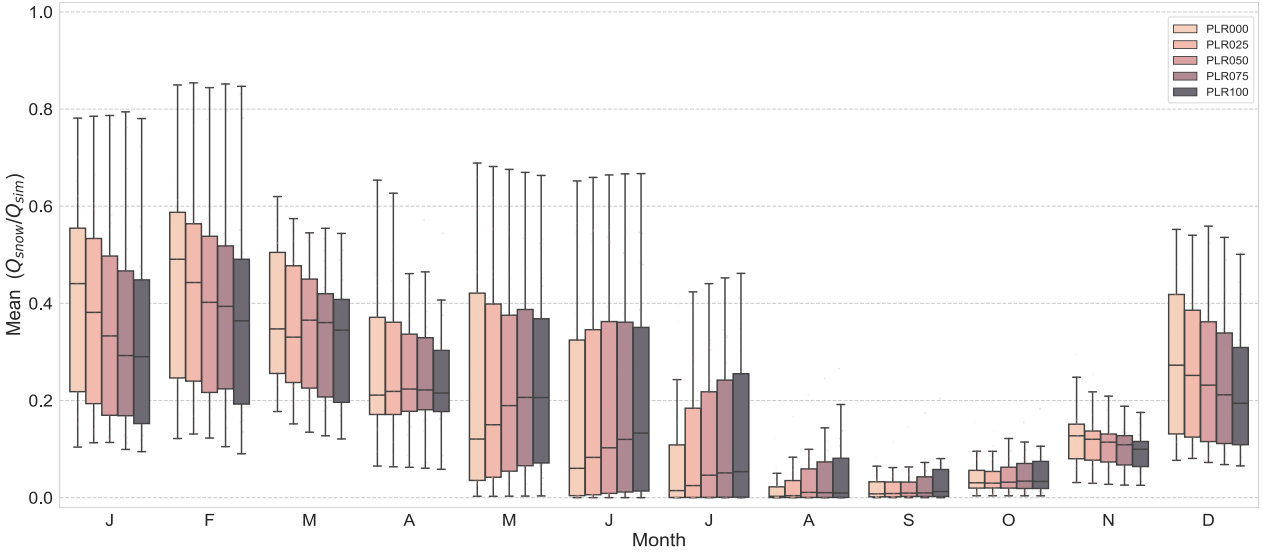

Figure 9 Mean fraction of runoff attributed to snowmelt per month.

4.6 Uncertainty

We then calculated uncertainty indicators to understand how the choice of PLR affects flood events across different return periods. The differences in medians, uncertainty ranges and confidence interval amplitudes (CIAs) between the AMFs from the baseline runs and those obtained with PLRs of 0%, 2.5%, 7.5% and 10% vary by return period and catchment (Fig. 10). Relative differences in median estimates and uncertainty ranges (Q_{95}-Q_{05}) are mostly negative when PLRs smaller than 5% were applied, whereas they are mostly positive when PLRs larger than 5% were applied. These relative differences are larger and more variable for PLRs of 0% and 10% compared to PLRs of 2.5% and 7.5%, and they show little variation with return period. In contrast, relative differences in the CIAs are larger for the 0% PLR compared to the other PLRs for nearly all return periods. Although these differences have a mean value close to zero, their variability decreases with increasing return period, indicating that the choice of the PLR has limited influence on the uncertainty of large floods.

https://doi.org/10.5194/egusphere-2026-2338
Preprint. Discussion started: 28 April 2026

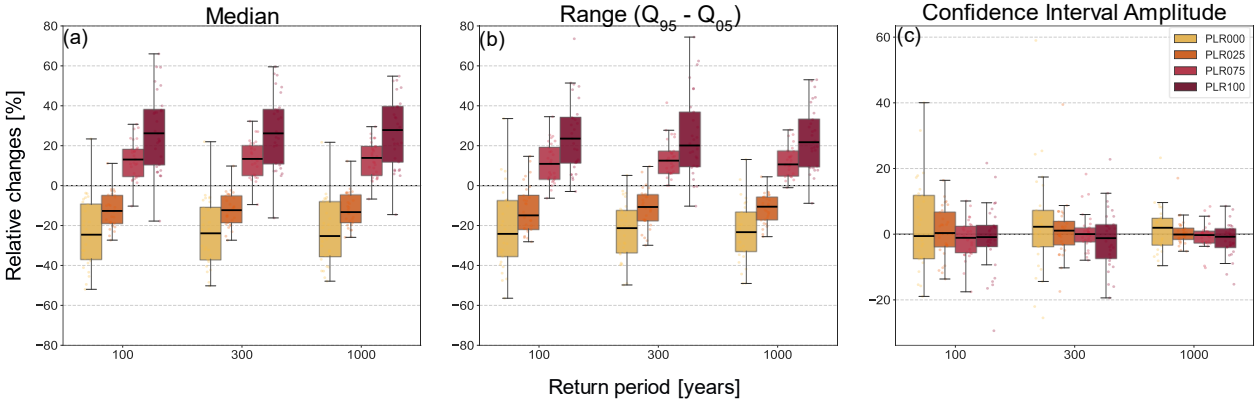

Figure 10 Relative difference between AMFs from baseline runs and AMFs under different PLRs: (a) medians; (b) uncertainty range (Q95 − Q05) and (c) confidence interval amplitude, each for return periods of 100, 300 and 1000 years across catchments (one point in the box plot represents one catchment).

4.7 The role of precipitation lapse rate in the hydrological model

We further investigated the impact of the internal lapse rate on flood estimates by considering only different values of PLR_HBV. The seasonal pattern remains consistent with that observed when both PLRs are changed consistently in the weather generator and hydrological model (cf. Figs. 7a,b,c,d and Fig. S1 in the Supplement). The main difference lies in the flood magnitudes, which were not substantially altered because precipitation input amounts were identical for all simulations. To explain this pattern, we examined the relationship between the mean absolute relative change in AMFs and the redistribution index (RI), which quantifies the importance of the hydrological model's precipitation redistribution across elevation zones within a catchment. For instance, the impact of a given lapse rate is expected to be smaller in a catchment with smaller elevation range ts compared to a catchment covering a larger elevation range. Consequently, the RI explains differences in simulated AMFs across the selected PLR_HBV values. Indeed, there is a clear linear positive relationship between RI and the mean relative change in AMFs (Fig. 11): catchments with a higher RI exhibit larger deviations in AMF compared to the 5% PLR_HBV. This relationship generally strengthens with increasing PLRs, but is strongest for the 7.5% PLR_HBV.

Furthermore, the relative differences in medians, uncertainty ranges, and CIAs were smaller when only the model internal PLR_HBV was varied. Specifically, the differences of the medians range between -5 and 15%, while these differences vary between -50 to 80% when both PLR were altered, indicating that only a small percentage of change in magnitude of floods is attributed to the internal change of lapse rate. Notably, the changes in median for PLR_HBV are mostly positive for all return periods and lapse rates. This highlights that not only increasing but also decreasing the internal lapse rate in the hydrological model leads to increases in the magnitude of certain floods, most likely the winter events (Fig. 12).

https://doi.org/10.5194/egusphere-2026-2338
Preprint. Discussion started: 28 April 2026

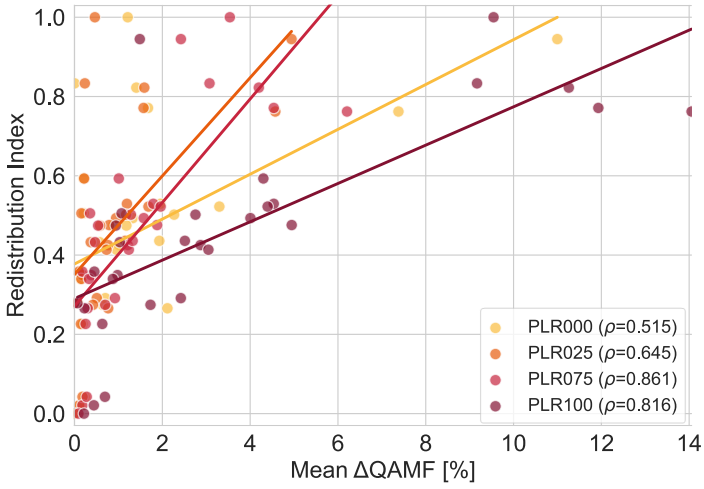

Figure 11 Relationship between the redistribution index and the change in mean AMFs simulated with PLR_HBV relative to the baseline. Each point represents one catchment and PLR_HBV.

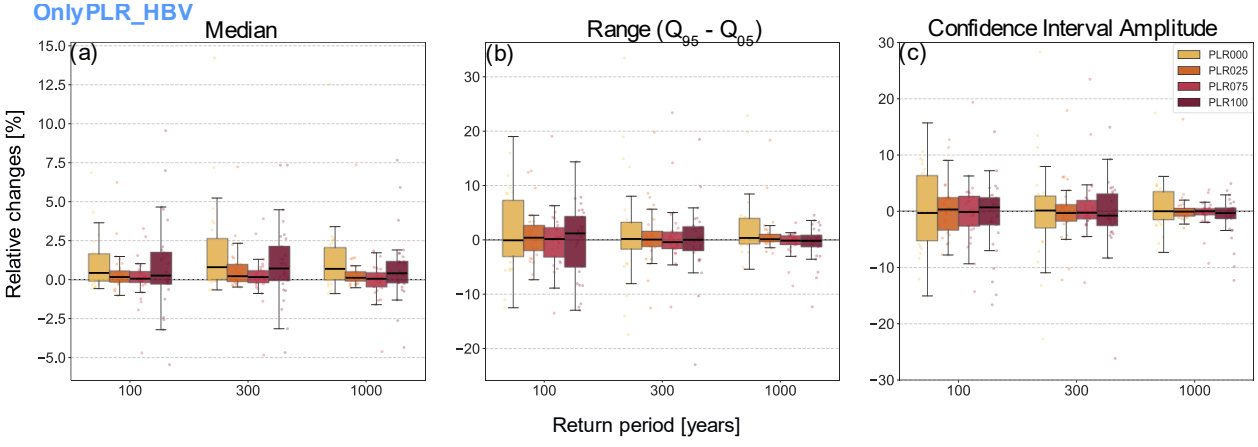

Figure 12 Relative difference between AMFs from baseline runs and AMFs under different values of the internal lapse rate used in HBV (PLR_HBV), where the lapse rate used for the weather generator (PLR_WG) was kept at 5%): (a) median; (b) uncertainty range (Q95 − Q05) and (c) confidence interval amplitude, each for return periods of 100, 300 and 1000 years across catchments (one point in the box plot represents one catchment).

5 Discussion

5.1 Effect of the precipitation lapse rate in the weather generator

The linear correlation between ΔElevation (mean catchment elevation minus the mean Thiessen-weighted station elevation) and differences in mean annual precipitation from the weather generator (calculated for 0%, 2.5%, 7.5%, and 10% relative to the baseline 5%) highlights the influence of the meteorological network on the generation of synthetic time series for each

https://doi.org/10.5194/egusphere-2026-2338
Preprint. Discussion started: 28 April 2026

catchment. In the weather generator, the lapse rate is applied to every station to adjust precipitation to the mean catchment elevation. When the mean catchment elevation deviates substantially from the elevations represented by the station network, the lapse rate adjustment amplifies precipitation discrepancies. These uncertainties are further modulated by station density and the length of the observational records used to parameterize the weather generator (see Kritidou et al. (2025) for details). In this context, it should be recalled that Switzerland is characterized by a dense meteorological station network, which covers intermediate elevations well, but underrepresents elevations above 1500 m a.s.l (Isotta et al., 2019; Viviroli et al., 2011). However, it should also be noted that ΔElevation decreases for catchments above 2500m, as some of these are small catchments with only a few high-elevation stations or are characterized by comparatively high station density.

5.2 Impact on runoff components

The sensitivity coefficients of the different runoff components show distinct seasonal and elevation-dependent patterns. The sensitivity coefficients of total simulated runoff were negatively correlated with elevation for all seasons and lapse rates: lower-elevation catchments are more sensitive to changes in lapse rates, whereas higher-elevation catchments are less sensitive. This can be explained by the dynamics of snow accumulation and melt processes in catchments at higher elevations (Barrera et al., 2020; Weiler et al., 2025) and the strong role of precipitation in snowpack variability above 1400 m a.s.l. (±200m) in the mountainous regions of Switzerland (Morán-Tejeda et al., 2013). The variability of snowpack is, however, less straightforward to detect in the snowmelt component because of the varying lag time between the snowfall and its release from the snowpack, which ultimately contributes to streamflow (Schaefli et al., 2013). In addition to seasonal snow storage, high-elevation catchments may contain important subsurface water stores (Cochand et al., 2019; Somers and McKenzie, 2020; Staudinger et al., 2017; Weiler et al., 2025). As a result, they can exhibit more pronounced memory effects than lower-elevation catchments (Floriancic et al., 2024; Jenicek et al., 2016, 2018). However, it remains challenging to determine the extent to which this storage effect can compensate for decreases in snow or ice storage due to a different PLR and delay the release of runoff downstream (Hale et al., 2023).

In winter, small lapse rates show higher sensitivity coefficients compared to larger ones. Precipitation contributes substantially to snowpack accumulation for lapse rates above 5%. However, for lapse rates below 5%, little or no snow accumulates at high elevations, and precipitation from lower elevations melts (Blanchet et al., 2009; Weiler et al., 2025) and increases the snowmelt. This is supported by the smaller area below the threshold elevation in winter (Fig. 4), as well as by the comparatively higher snowmelt fraction of the annual maxima (Fig. 9). A decrease in snowmelt with increasing precipitation has been associated with low or even negative elasticities (i.e., sensitivity of streamflow to changes in precipitation) in high-elevation catchments (Li et al., 2020). Additionally, wet antecedent conditions as maximum soil moisture (Pellet and Hauck, 2016), often coincide with snowmelt (Harpold and Molotch, 2015).

In spring, the sensitivity coefficients of lapse rates and runoff components show high variability, reflecting the nonlinear responses of runoff to changes in precipitation (see also Fig. 6). An increase in the area below threshold elevation from March to May indicates a transition from more snow to more rain due to rising temperatures. At elevations below 1800 m a.s.l., lapse

https://doi.org/10.5194/egusphere-2026-2338
Preprint. Discussion started: 28 April 2026

rates lower than 5% generally exhibit smaller runoff sensitivity coefficients compared to those above 5%. This relationship reverses at higher elevations (> 1800 m a.s.l.) due to the increasing importance of snow accumulation.

In summer, the sensitivity coefficients of all runoff components are relatively higher compared to other seasons, except for the glacier component. This is attributed to the strong seasonality of the catchments: most receive more precipitation in summer than in winter, often in the form of high-intensity events that generate direct runoff in both lower- and higher-elevation catchments. Weiler et al. (2025) found the highest weekly summer streamflow sensitivities to precipitation at high elevations in Switzerland, supporting our argument for a more direct runoff response. However, the authors found low sensitivities at lower-elevation catchments when calculated on a weekly basis, making a direct comparison with the seasonal values difficult. In summer, the lower elasticities observed for high-elevation catchments could be linked to higher soil moisture (Sankarasubramanian et al., 2001), which generally increases with elevation in Switzerland (up to 2000 m a.s.l.) (Pellet and Hauck, 2016), as well as to the key role of snow processes (Sankarasubramanian et al., 2001).

In autumn, higher sensitivity coefficients are associated with higher precipitation lapse rates, extending to nearly 1800 m a.s.l. for both rainfall and snowmelt runoff. During this season, most of the precipitation falls as rain (Fig. 4). In November, some snowfall occurs, which melts rather quickly (Weiler et al., 2025) and likely increases the snowmelt contribution. As a result, lower-elevation catchments convert precipitation into direct runoff and show higher sensitivity to changes in lapse rate.

Negative sensitivity coefficients for glacier runoff can be explained by the fact that glaciers are more sensitive to temperature changes than precipitation, especially in summer (Weiler et al., 2025). Strongly glaciated areas are associated with negative runoff responses, as only 30% of the amplitude in precipitation variability translates into runoff variability (Pohl et al., 2017). Additionally, snow protects the glacier from melting. More precipitation in the form of snow can therefore result in less glacier melt. Note that the number of glaciated catchments considered in our study is small, and that the relationship between sensitivity coefficients and elevation is not statistically significant. This limits our understanding of how changes in precipitation amount can affect the glacier melt runoff.

These findings are further confirmed by the relative changes in simulated runoff per season (Fig 6). Depending on the season and lapse rate, seasonal runoff changes resulted in either additive or counteracting effects. Larger relative changes are attributed to the larger change in precipitation amount (0% and 10% PLR) and are also reflected in the uncertainties in annual maximum floods (Fig. 10). Although a systematic link between mean catchment elevation and the seasonal or annual relative change in runoff could not be identified, it is noteworthy that some of the high elevation catchments exhibit small relative changes, supporting our finding that they might be less sensitive to variation of the PLRs. In some catchments, an increase in precipitation in winter and spring even led to a decrease in simulated runoff (Fig. 6). This variable response of the different runoff components may be explained by changes in the snowfall fraction, an important indicator of changes in annual runoff (Barnhart et al., 2016; Berghuijs et al., 2014). These observations are consistent with prior modelling and empirical studies showing that snowpack accumulation and snowmelt respond differently to changes in precipitation magnitude depending on catchment characteristics (Barnhart et al., 2016; Knowles et al., 2006; Luce et al., 2014). In the Tarim River Basin, for instance, some streams were found to be more sensitive to precipitation, while others were more sensitive to temperature (He et al.,

https://doi.org/10.5194/egusphere-2026-2338
Preprint. Discussion started: 28 April 2026

2025; Weiler et al., 2025). Although elevation was found to exert a major control on runoff-component sensitivity, other climate variables (Tang et al., 2019; Zhang et al., 2022), temporal scales (Andréassian et al., 2016) and factors such as runoff coefficients (Hunt et al., 2023) or humidity index (Zhang et al., 2022) may also help explain the observed sensitivity coefficients. Sensitivity coefficients derived from hydrological simulations inherently reflect model complexities (Zhang et al., 2022). In our study, they represent the combined effects of the lapse rate adjustments in the weather generator and the hydrological model.

5.3 Seasonality and magnitude of extremes

A shift towards more winter floods occurred when the lapse rate was reduced below 5%, whereas higher lapse rates led to more summer floods (Fig. 7 and Fig. S2). In alpine catchments, the annual maximum flood typically occurs in summer due to high rainfall intensities, typically combined with a high snowline or additional melting processes (Muelchi et al., 2021), while winter represents the low-flow season (Brunner and Slater, 2022). Reducing the lapse rate increases the snowmelt contribution in winter (Fig. 9). This suggests that floods occurring in winter and early spring result from a combination of liquid precipitation and potential earlier snowmelt. In typical mountainous catchments, winter floods usually involve rain-on-snow processes, where antecedent snowmelt saturates the soils and even relatively low rainfall intensities can still produce floods (Beniston and Stoffel, 2016). These results are consistent with previous studies highlighting soil moisture as a key driver of flood generation mechanisms, indicating that precipitation alone cannot fully explain the observed changes in flood occurrence (Bales et al., 2006; Bertola et al., 2021; Harpold and Molotch, 2015; Wasko and Nathan, 2019).

When only the internal lapse rate in the hydrological model was altered, the shift in flood seasonality was identical, whereas flood magnitudes did not change markedly. Winter floods under small lapse rates were comparable to, and in some cases even larger than, those under higher lapse rates. This underscores that changes in flood mechanisms arise from the model-internal adjustment of the lapse rate, and that these effects can be amplified depending on catchment characteristics (i.e., a high redistribution index; Fig. 11). Spring and summer floods are associated with a combination of high precipitation intensities and snowmelt. In our experimental setup, increasing the precipitation amounts fed into the hydrological model and redistributing them across elevation zones with a higher internal lapse rate resulted in greater snow accumulation at higher elevations. This snowpack is subsequently retained and melts during the summer months, with higher lapse rates leading to a larger snowmelt contribution (Fig. 9). This also explains why the 0% PLR produces most low-magnitude floods in winter, whereas in summer both flood frequency and magnitude increase linearly with PLR.

While clear patterns of change have been detected for flood timing, changes in flood magnitude are strongly influenced by antecedent conditions, which determine the fraction of rainfall converted into direct runoff (Berghuijs et al., 2016; Nied et al., 2017). From the two example catchments presented, we can hypothesize that snowmelt-dominated catchments (e.g., Sarine) are more sensitive to the change in lapse rate compared to rainfall-dominated catchments (e.g., Maggia) in both experimental set-ups. This may be explained by the strong influence of changes in precipitation phase (rain or snow), although other factors such as catchment size, topography, and total precipitation amount may also contribute to the observed changes in magnitude.

https://doi.org/10.5194/egusphere-2026-2338
Preprint. Discussion started: 28 April 2026

5.4 Uncertainty

We grouped the annual maxima from all PLRs by return period and quantified the corresponding uncertainties relative to the baseline lapse rate (5%). A key strength of our approach is that we sample flood events derived from very long synthetic time series, which allows us to examine very rare extremes (up to 1000-year events) for each experiment that are not captured in the relatively short observed time series. Additionally, this comparative analysis allows us to better understand how certain choices in hydrological modelling studies influence runoff simulations and specifically the extremes.

Both in the coupled change of PLR_GWEX and PLR_HBV and the isolated change of PLR_HBV, the CIA decreased with increasing PLR and return period. This may reflect changes in flood generation mechanisms. As discussed earlier, a reduction in PLR leads to a shift towards winter floods. These events are typically smaller in magnitude as precipitation input was altered and are therefore associated with smaller return periods. In contrast, large floods occur mainly in summer and correspond to higher return periods. Thus, adjustments to the lapse rate primarily affect flood events with smaller return periods, while larger events the flood-generating processes are less impacted. This finding aligns with the lower sensitivity of high-elevation catchments to changes in precipitation. However, higher-elevation catchments often show larger heterogeneity of landscape features than lower-elevation catchments and present higher heterogeneity of the flood-generating processes. For instance, snowmelt floods show higher variability in terms of durations compared to synoptic or flash floods (see Gaál et al. (2015) for details). Gaál et al. (2015) also reported that the similarity of flood generation processes, as determined by the consistency of flood peak-volume relationships, decreases with an increasing snow-to-precipitation ratios and stronger flood seasonality. Reducing the lapse rate weakens this seasonality, whereas increasing the lapse rate does not substantially alter it. In the winter months, the snow-to-precipitation ratio increases as the lapse rate decreases, suggesting greater process variability. This variability appears more relevant for decreasing lapse rates than increasing ones, and more relevant for lower- elevation catchments than for higher-elevation catchments.

The variability of flood occurrence is larger for small return periods than for large return periods (Fig 8), indicating that changes in the lapse rate tend to change the seasonal timing of small floods, whereas large floods tend to retain their strong seasonal pattern. Snowmelt and rain-on-snow floods in low-elevation catchments can lead to highly variable hydrographs because moderate rainfall events may coincide with high baseflow generated (Gaál et al., 2015). Memory effects of hydrological systems may further contribute to this variability. For example, catchments dominated by summer floods and exhibiting strong seasonality show greater dependence between ensemble members than winter floods (Brunner and Slater, 2022). Ultimately, our findings emphasize the critical role of the lapse rate – both in the weather generator and in the hydrological model – in shaping flood seasonality and magnitude, and in influencing runoff generation processes.

https://doi.org/10.5194/egusphere-2026-2338
Preprint. Discussion started: 28 April 2026

5.5 Limitations

5.5.1 Linear and positive lapse rate

In this study, we varied the lapse rates, but always assumed them to be linear and positive. However, in topographically complex regions such as Switzerland, precipitation-elevation relationships are often non-monotonic, showing increasing-decreasing patterns (He et al., 2025). Lapse rates vary within individual mountain regions (Pepin et al., 2022) and depend on season (Benoit et al., 2024), topography and atmospheric factors (Napoli et al., 2019). In the Alps, annual precipitation generally increases with elevation up to 800–1000 m a.s.l., after which a saturation-like behaviour in orographic enhancement is observed (Napoli et al., 2019). This saturation effect was also highlighted by Blanchet et al. (2009) for mean and maximum snowfall across Switzerland, while a reverse orographic effect was identified for short-duration annual maximum precipitation by Avanzi et al. (2015). Overall, only 15% of observed cases corresponded to a linear and positive lapse rate (Benoit et al., 2024). Therefore, assuming a constant lapse rate is insufficient to describe the elevation-dependent orographic effects over the full simulation period (Hublart and Ruelland, 2016) and may lead to unrealistic flood simulations (Hingray et al., 2010; Legrand et al., 2024). The representation of precipitation-elevation dependency in this study is thus a simplification of the underlying physical processes. Future work should therefore aim to implement more flexible and regionally varying precipitation-elevation relationships in both the weather generator and the hydrological model, allowing for local gradients and small-scale variability.

5.5.2 Precipitation input

When interpreting the results, the uncertainties in precipitation input due to differences in network density and observation length should be kept in mind. As pointed out in the introduction, observational networks at high elevations are less dense than to those at lower elevations, making us “largely blind” about the conditions of these high-elevation regions (Dettinger, 2014). Uncertainties in precipitation products due to insufficient network density – including spatial, temporal and elevation-related uncertainties (Bertoncini and Pomeroy, 2025b) – propagate through hydrological models (Zhou et al., 2021b; Bárdossy et al., 2022a; Bárdossy and Anwar, 2023; Stephens and Bledsoe, 2023; Zhou et al., 2021a) and may lead to under- or overestimation of runoff (Brunner and Slater, 2022), as well as amplification of extremes (Kritidou et al., 2025). Even for catchments with a representative station network, precipitation can account for up to 50% of uncertainty in runoff simulations (Bárdossy et al., 2022b). Furthermore, the weather generator employed in this study is a powerful tool suitable for large river basins, but it is not designed to capture high-intensity, localized events that occur at sub-hourly resolution (Evin et al., 2019; Kritidou et al., 2025, 2026; Viviroli et al., 2022). Despite their relevance for small alpine catchments, they are likely not reliably simulated.

https://doi.org/10.5194/egusphere-2026-2338
Preprint. Discussion started: 28 April 2026

5.5.3 Hydrological modelling

Several sources of uncertainty in runoff simulations originate from the hydrological model. However, the plausibility of simulated extremes relies on the representation of hydrological processes and their drivers in the hydrological model. A critical component of these processes is the partitioning of precipitation into rain or snow. In the HBV model, precipitation at each elevation and vegetation zone is classified as either rain or snow using a threshold temperature, and the snowfall amount is subsequently multiplied by a snowfall correction factor, SFCF. This is a simplified conceptualization that does not account for a transition between precipitation phases and can lead to errors in the representation of spring snowmelt dynamics (Harder and Pomeroy, 2013; Mizukami et al., 2013). Recent efforts have been made to incorporate more complex phase partitioning methods (Jennings and Molotch, 2019; Singh et al., 2024) and more detailed descriptions of snow processes (Gallice et al., 2016; Lehning et al., 2006; Quéno et al., 2024). For instance, Singh et al. 2024 found that moving from a static to a dynamically variable precipitation phase partitioning approach increased snowmelt contribution to runoff by 8%. Additionally, although we use a time-varying and regionally specific temperature lapse rate, a deterministic relationship between air temperature and precipitation phase is assumed in the hydrological model. Other factors, such as relative humidity, are not taken into account, potentially leading to errors in phase characterization for individual events and resulting in notable differences in flood simulations (Froidurot et al., 2014; Hingray et al., 2010).

Although the parameters of the snow routine are useful for gauge undercatch correction (Staudinger et al., 2025) and for adapting to catchment snow processes (Ruelland, 2020), the extent to which these adjustments occur varies with catchment hypsography (see for example the influence of the redistribution index in Fig. 11). Adding more detail to the snow routine model structure did not markedly improve simulations of snow water equivalent and runoff when several mountainous catchments in Switzerland and Czeck Republic were examined (Girons Lopez et al., 2020b). However, context- and region-dependent adaptations would be valuable to understand the extent to which the parameters of the snow routine compensate for errors in precipitation inputs (Ruelland, 2020). This might be particularly critical for small alpine catchments.

5.5.4 Methodological choices

We applied a one-at-a-time sensitivity analysis, varying only the precipitation lapse parameter of the HBV model while keeping all other parameters constant. Although this is a valuable approach for isolating the impact of individual parameters on hydrological simulations, it does not capture the complex interactions and interdependencies between parameters, nor the compensation effects that would emerge if the hydrological model were recalibrated for each precipitation input. However, this exploration was beyond the scope of this study.

We also performed our sensitivity analysis by using a benchmark for comparison. This benchmark is based on previous work that used the same modelling chain with a constant lapse rate and produced reasonable flood estimates. However, this approach was subject to some limitations and uncertainties, including under- or overestimation of floods in specific catchments. Thus, while we did not identify any “better” lapse rate with clear physical meaning for each catchment, we provide information on

https://doi.org/10.5194/egusphere-2026-2338
Preprint. Discussion started: 28 April 2026

how methodological choices influence the results. Given that most hydrological models represent complex processes in a simplified manner, some assumptions are unavoidable. However, further investigation is still needed to assess whether improved process understanding and representation could lead to practical guidance for improving precipitation lapse rates in hydrological models, or whether the limited length, representativeness and homogeneity of meteorological data are the main drivers for this lack of understanding.

Furthermore, it should be noted that event selection based on annual maximum discharge can introduce bias, as events with wetter antecedent conditions may lead to spuriously large flood responses (Wasko and Guo, 2022). Although this introduces uncertainties related to rainfall-runoff response, it still sheds light on the underlying processes triggered by the choice of a specific lapse rate.

Lastly, our study assumes a stationary climate. However, projected changes in precipitation characteristics in the Alps are expected to increase the risk of flash floods (Estermann et al., 2025) as well as rain-on-snow events (Beniston and Stoffel, 2016). Of particular importance is the intensification of heavy precipitation events, as those events are critical for infrastructure safety (Prein et al., 2017; Vergara-Temprado et al., 2021).

6 Conclusions

In this study, we explored the impact of precipitation lapse rate on runoff simulations, focusing on mean annual and seasonal runoff as well as annual maximum floods for several catchments in Switzerland. We focused on typical mountainous catchments, where lapse rates are key drivers of precipitation behaviour and where our understanding remains limited due to the spatiotemporal coverage of the station network. The simulations were performed by driving a hydrological model with long synthetic time series of precipitation from a stochastic weather generator. The lapse rate in the weather generator modifies the precipitation amounts, whereas the lapse rate in the hydrological model modifies the distribution of precipitation with elevation.

We found that rain, snow, and glacier runoff components were sensitive to changes in the amount and distribution of precipitation within the catchment induced by changes in lapse rate. Overall, a 10% change in precipitation led to a 4–20% change in simulated runoff depending on the catchment, season, and lapse rate. Lower-elevation catchments showed a stronger sensitivity than higher-elevation ones. Lapse rates below 5% also led to more variable runoff responses than higher values. This variability was influenced by precipitation magnitude and by the redistribution index in the hydrological model.

Changes in simulated flood seasonality were more influenced to a larger extent by the internal lapse rate in the hydrological model. However, changes in flood magnitude were mainly driven by changes in precipitation amount, influenced by the lapse rate in the weather generator. Lower lapse rates increased the snowmelt contribution and the number of floods in winter, whereas higher lapse rates increased the snowmelt contribution and the number of floods in summer.

Furthermore, we found that the seasonality of frequent floods was more sensitive to the choice of precipitation lapse rate than of extreme, rare events, which tend to retain their strong seasonality. When both lapse rates were altered, the relative differences

https://doi.org/10.5194/egusphere-2026-2338
Preprint. Discussion started: 28 April 2026

in flood medians, uncertainty ranges, and confidence interval amplitudes compared to the baseline varied between -50% and 70%, -55% and 80%, and-20% and-40%, respectively. When only the internal lapse rate was altered, the relative differences in flood medians, uncertainty ranges, and confidence interval amplitudes compared to the baseline varied between -5% and 15%, -25% and 35%, and -25% and 30%, respectively, underscoring the influence of the amount of precipitation input.

Overall, the runoff responses and their corresponding uncertainties highlight two distinct yet interacting controls: mean catchment precipitation and its redistribution within the hydrological model. The spatiotemporal coverage of the observation network influences these uncertainties and limits the understanding of the relationship between precipitation and elevation. Improvements would be expected from expanding current observation networks, but also from the use of weather radar data or remotely sensed snow-cover observations to calibrate and validate hydrological models. Additional valuable data sources would be glacier mass balance observations and inflow estimates for reservoirs. Future work should therefore focus on integrating such observations into hydrological modelling frameworks.

Furthermore, our results highlight the need for a more realistic representation of precipitation dynamics in the hydrological models, particularly in regions where snow-to-rain transitions are important. The simplified assumptions of a linear, constant lapse rate, is commonly applied, even across catchments with different physiographic characteristics, but is often not critically evaluated in hydrological studies. Although our study relies on a synthetic experiment with modelling choices that strongly simplify snow-rain partitioning, it demonstrates the impact of these common assumptions on runoff simulations. We thus suggest that moving towards more flexible precipitation-elevation relationships may have important implications for understanding the water balance, in particular for high-elevation catchments. Future efforts are needed to integrate detailed snowpack models and precipitation phase-partitioning approaches to better distinguish between rain and snow and to quantify their relative contributions to simulated runoff.

Ultimately, our results highlight methodological constraints, representing a first step towards model improvement and contributing to a broader scientific discourse. Such improvements would be important to support decision-making related to reservoir storage, downstream agricultural irrigation, and flood risk management. This is because the value of hydrological models is not limited to their ability to provide reliable runoff simulations but also lies in the systematic examination of associated uncertainties. Our results may also be transferable to other regions with similar climatological conditions; however, it should be kept in mind that the framework used here is governed by additional factors, including precipitation magnitude and seasonality as well as topographic characteristics.

Code and data availability

Code used in this project and resulting data can be obtained from the first author upon reasonable request. The links to the meteorological data, discharge observations, weather generator, and hydrological model are provided below. However, the very large volume of data produced in this study, combined with the complex data organization across collaborating groups, makes it difficult to make all datasets publicly accessible. Likewise, the code used for data processing, post-processing,

https://doi.org/10.5194/egusphere-2026-2338
Preprint. Discussion started: 28 April 2026

modelling, and evaluation consists of numerous partially interdependent components that have been developed and adapted over the last years. Preparing these workflows for public release would require extensive curation, documentation, and generalization, efforts that are beyond the available resources for the current study. Together with the federal offices funding the project, work has been initiated to curate selected datasets for a public database, but the substantial effort involved means that these will not be available in the near future.

The meteorological data from MeteoSwiss:
https://github.com/MeteoSwiss/opendata/blob/main/README.md

The discharge data from the Federal Office fort he Environment:
https://www.bafu.admin.ch/de/datenservice-hydrologie-fuer-fliessgewaesser-und-seen

The weather generator:
https://cran.r-project.org/web/packages/GWEX/GWEX.pdf

The HBV model:
https://www.geo.uzh.ch/en/units/h2k/Services/HBV-Model/HBV-Download.html

Author contributions

EK, DV and MS designed the experiments. GE developed the weather generator. EK performed the simulations, visualized and investigated the results. EK prepared the original manuscript which was reviewed and edited by all co-authors.

Competing interests

At least one of the authors is a member of the editorial board of *Hydrology and Earth System Sciences*.

Acknowledgements

We thank Benoit Hingray for contributions to the generation of the GWEX scenarios and insightful comments on the manuscript.

Financial support

This research has been supported by the Federal Office for the Environment FOEN and the Swiss Federal Office of Energy SFOE as a part of the project “Extreme Floods in Switzerland” (EXCH).

https://doi.org/10.5194/egusphere-2026-2338
Preprint. Discussion started: 28 April 2026

References

Akhtar, M., Ahmad, N., and Booij, M. J.: Use of regional climate model simulations as input for hydrological models for the Hindukush-Karakorum-Himalaya region, Hydrol. Earth Syst. Sci., 2009.

Al-Safi, H. I. J. and Sarukkalige, P. R.: The application of conceptual modelling to assess the impacts of future climate change on the hydrological response of the Harvey River catchment, Journal of Hydro-environment Research, 28, 22–33, https://doi.org/10.1016/j.jher.2018.01.006, 2020.

Andréassian, V., Coron, L., Lerat, J., and Le Moine, N.: Climate elasticity of streamflow revisited – an elasticity index based on long-term hydrometeorological records, Hydrol. Earth Syst. Sci., 20, 4503–4524, https://doi.org/10.5194/hess-20-4503-2016, 2016.

Arnaud, P., Cantet, P., and Odry, J.: Uncertainties of flood frequency estimation approaches based on continuous simulation using data resampling, Journal of Hydrology, 554, 360–369, https://doi.org/10.1016/j.jhydrol.2017.09.011, 2017.

Avanzi, F., De Michele, C., Gabriele, S., Ghezzi, A., and Rosso, R.: Orographic Signature on Extreme Precipitation of Short Durations, Journal of Hydrometeorology, 16, 278–294, https://doi.org/10.1175/JHM-D-14-0063.1, 2015.

Avanzi, F., Ercolani, G., Gabellani, S., Cremonese, E., Pogliotti, P., Filippa, G., Morra Di Cella, U., Ratto, S., Stevenin, H., Cauduro, M., and Juglair, S.: Learning about precipitation orographic enhancement from snow-course data improves water-balance modeling, https://doi.org/10.5194/hess-2020-571, 26 November 2020.

Bales, R. C., Molotch, N. P., Painter, T. H., Dettinger, M. D., Rice, R., and Dozier, J.: Mountain hydrology of the western United States, Water Resources Research, 42, 2005WR004387, https://doi.org/10.1029/2005WR004387, 2006.

Bárdossy, A. and Anwar, F.: Why do our rainfall–runoff models keep underestimating the peak flows?, Hydrol. Earth Syst. Sci., 27, 1987–2000, https://doi.org/10.5194/hess-27-1987-2023, 2023.

Bardossy, A. and Das, T.: Influence of rainfall observation network on model calibration and application, Hydrol. Earth Syst. Sci., 2008.

Bárdossy, A., Kilsby, C., Birkinshaw, S., Wang, N., and Anwar, F.: Is Precipitation Responsible for the Most Hydrological Model Uncertainty?, Front. Water, 4, 836554, https://doi.org/10.3389/frwa.2022.836554, 2022a.

Bárdossy, A., Kilsby, C., Birkinshaw, S., Wang, N., and Anwar, F.: Is Precipitation Responsible for the Most Hydrological Model Uncertainty?, Front. Water, 4, 836554, https://doi.org/10.3389/frwa.2022.836554, 2022b.

Barnhart, T. B., Molotch, N. P., Livneh, B., Harpold, A. A., Knowles, J. F., and Schneider, D.: Snowmelt rate dictates streamflow, Geophysical Research Letters, 43, 8006–8016, https://doi.org/10.1002/2016GL069690, 2016.

Barrera, C., Núñez Cobo, J., Souvignet, M., Oyarzún, J., and Oyarzún, R.: Streamflow elasticity, in a context of climate change, in arid Andean watersheds of north-central Chile, Hydrological Sciences Journal, 65, 1707–1719, https://doi.org/10.1080/02626667.2020.1770764, 2020.

Barry, R. G. and Chorley, R. J.: Atmosphere, weather and climate, 9. ed., Routledge, London, 516 pp., 2010.

Bell, B. A., Hughes, P. D., Fletcher, W. J., Cornelissen, H. L., Rhoujjati, A., Hanich, L., and Braithwaite, R. J.: Climate of the Marrakech High Atlas, Morocco: Temperature lapse rates and precipitation gradient from piedmont to summits, Arctic, Antarctic, and Alpine Research, 54, 78–95, https://doi.org/10.1080/15230430.2022.2046897, 2022.

https://doi.org/10.5194/egusphere-2026-2338
Preprint. Discussion started: 28 April 2026

Beniston, M. and Stoffel, M.: Rain-on-snow events, floods and climate change in the Alps: Events may increase with warming up to 4 °C and decrease thereafter, Science of The Total Environment, 571, 228–236, https://doi.org/10.1016/j.scitotenv.2016.07.146, 2016.

Benoit, L., Koch, E., Peleg, N., and Mariethoz, G.: Precipitation-elevation relationship: Non-linearity and space–time variability prevail in the Swiss Alps, Journal of Hydrology X, 25, 100186, https://doi.org/10.1016/j.hydroa.2024.100186, 2024.

Bergström, S.: THE HBVMODEL - its structure and applications, 1992.

Bertola, M., Viglione, A., Vorogushyn, S., Lun, D., Merz, B., and Blöschl, G.: Do small and large floods have the same drivers of change? A regional attribution analysis in Europe, Hydrol. Earth Syst. Sci., 25, 1347–1364, https://doi.org/10.5194/hess-25-1347-2021, 2021.

Bertoncini, A. and Pomeroy, J. W.: Quantifying spatiotemporal and elevational precipitation gauge network uncertainty in the Canadian Rockies, Hydrol. Earth Syst. Sci., 29, 983–1000, https://doi.org/10.5194/hess-29-983-2025, 2025a.

Bertoncini, A. and Pomeroy, J. W.: Quantifying spatiotemporal and elevational precipitation gauge network uncertainty in the Canadian Rockies, Hydrol. Earth Syst. Sci., 29, 983–1000, https://doi.org/10.5194/hess-29-983-2025, 2025b.

Blanchet, J., Marty, C., and Lehning, M.: Extreme value statistics of snowfall in the Swiss Alpine region, Water Resources Research, 45, 2009WR007916, https://doi.org/10.1029/2009WR007916, 2009.

Bohne, L., Strong, C., and Steenburgh, W. J.: Climatology of Orographic Precipitation Gradients in the Contiguous Western United States, Journal of Hydrometeorology, 21, 1723–1740, https://doi.org/10.1175/JHM-D-19-0229.1, 2020.

Brunner, M. I. and Slater, L. J.: Extreme floods in Europe: going beyond observations using reforecast ensemble pooling, Hydrol. Earth Syst. Sci., 26, 469–482, https://doi.org/10.5194/hess-26-469-2022, 2022.

Budhathoki, B. R., Adhikari, T. R., Shrestha, S., and Awasthi, R. P.: Application of hydrological model to simulate streamflow contribution on water balance in Himalaya river basin, Nepal, Front. Earth Sci., 11, 1128959, https://doi.org/10.3389/feart.2023.1128959, 2023.

Buzzi, A., Tartaglione, N., and Malguzzi, P.: Numerical Simulations of the 1994 Piedmont Flood: Role of Orography and Moist Processes, Mon. Wea. Rev., 126, 2369–2383, https://doi.org/10.1175/1520-0493(1998)126<2369:NSOTPF>2.0.CO;2, 1998.

Chen, J. and Shi, X.: Quantifying Global Warming Response of the Orographic Precipitation in a Typhoon Environment with Large-Eddy Simulations, JOURNAL OF CLIMATE, 36, 2023.

Clerc-Schwarzenbach, F. and Do Nascimento, T. V. M.: Evaluating E-OBS forcing data for large-sample hydrology using model performance diagnostics, Hydrol. Earth Syst. Sci., 30, 119–140, https://doi.org/10.5194/hess-30-119-2026, 2026.

Clerc-Schwarzenbach, F., Selleri, G., Neri, M., Toth, E., Van Meerveld, I., and Seibert, J.: Large-sample hydrology – a few camels or a whole caravan?, Hydrol. Earth Syst. Sci., 28, 4219–4237, https://doi.org/10.5194/hess-28-4219-2024, 2024.

Clerc-Schwarzenbach, F., Seibert, J., Vis, M., and Van Meerveld, I.: Value of water level class observations for parameter set selection in hydrological modelling, Hydrological Sciences Journal, 70, 1464–1480, https://doi.org/10.1080/02626667.2025.2489994, 2025.

https://doi.org/10.5194/egusphere-2026-2338
Preprint. Discussion started: 28 April 2026

Cochand, M., Christe, P., Ornstein, P., and Hunkeler, D.: Groundwater Storage in High Alpine Catchments and Its Contribution to Streamflow, Water Resources Research, 55, 2613–2630, https://doi.org/10.1029/2018WR022989, 2019.

Crochet, P.: Enhancing radar estimates of precipitation over complex terrain using information derived from an orographic precipitation model, Journal of Hydrology, 377, 417–433, https://doi.org/10.1016/j.jhydrol.2009.08.038, 2009.

Daly, C., Neilson, R. P., and Phillips, D. L.: A Statistical-Topographic Model for Mapping Climatological Precipitation over Mountainous Terrain, J. Appl. Meteor., 33, 140–158, https://doi.org/10.1175/1520-0450(1994)033<0140:ASTMFM>2.0.CO;2, 1994.

Daly, C., Halbleib, M., Smith, J. I., Gibson, W. P., Doggett, M. K., Taylor, G. H., Curtis, J., and Pasteris, P. P.: Physiographically sensitive mapping of climatological temperature and precipitation across the conterminous United States, Intl Journal of Climatology, 28, 2031–2064, https://doi.org/10.1002/joc.1688, 2008.

Dettinger, M.: Impacts in the third dimension, Nature Geosci, 7, 166–167, https://doi.org/10.1038/ngeo2096, 2014.

Dettinger, M., Redmond, K., and Cayan, D.: Winter Orographic Precipitation Ratios in the Sierra Nevada—Large-Scale Atmospheric Circulations and Hydrologic Consequences, Journal of Hydrometeorology, 5, 1102–1116, https://doi.org/10.1175/JHM-390.1, 2004.

Driessen, T. L. A.: The hydrological response of the Ourthe catchment to climate change as modelled by the HBV model, Hydrol. Earth Syst. Sci., 2010.

Dura, V., Evin, G., Favre, A.-C., and Penot, D.: Spatial variability in the seasonal precipitation lapse rates in complex topographical regions – application in France, Hydrol. Earth Syst. Sci., 28, 2579–2601, https://doi.org/10.5194/hess-28-2579-2024, 2024.

Esmaeili-Gisavandani, H., Lotfirad, M., Sofla, M. S. D., and Ashrafzadeh, A.: Improving the performance of rainfall-runoff models using the gene expression programming approach, Journal of Water and Climate Change, 12, 3308–3329, https://doi.org/10.2166/wcc.2021.064, 2021.

Estermann, R., Rajczak, J., Velasquez, P., Lorenz, R., and Schär, C.: Projections of Heavy Precipitation Characteristics Over the Greater Alpine Region Using a Kilometer–Scale Climate Model Ensemble, JGR Atmospheres, 130, e2024JD040901, https://doi.org/10.1029/2024JD040901, 2025.

Evin, G., Favre, A.-C., and Hingray, B.: Stochastic generation of multi-site daily precipitation focusing on extreme events, Hydrol. Earth Syst. Sci., 22, 655–672, https://doi.org/10.5194/hess-22-655-2018, 2018.

Evin, G., Favre, A.-C., and Hingray, B.: Stochastic generators of multi-site daily temperature: comparison of performances in various applications, Theor Appl Climatol, 135, 811–824, https://doi.org/10.1007/s00704-018-2404-x, 2019.

Floriancic, M. G., Stockinger, M. P., Kirchner, J. W., and Stumpp, C.: Monthly new water fractions and their relationships with climate and catchment properties across Alpine rivers, Hydrol. Earth Syst. Sci., 28, 3675–3694, https://doi.org/10.5194/hess-28-3675-2024, 2024.

Foehn, A., García Hernández, J., Schaefli, B., and De Cesare, G.: Spatial interpolation of precipitation from multiple rain gauge networks and weather radar data for operational applications in Alpine catchments, Journal of Hydrology, 563, 1092–1110, https://doi.org/10.1016/j.jhydrol.2018.05.027, 2018.

https://doi.org/10.5194/egusphere-2026-2338
Preprint. Discussion started: 28 April 2026

Foresti, L. and Pozdnoukhov, A.: Exploration of alpine orographic precipitation patterns with radar image processing and clustering techniques, Meteorological Applications, 19, 407–419, https://doi.org/10.1002/met.272, 2012.

Frei, C. and Schär, C.: A precipitation climatology of the Alps from high-resolution rain-gauge observations, Int. J. Climatol., 18, 873–900, https://doi.org/10.1002/(SICI)1097-0088(19980630)18:8<873::AID-JOC255>3.0.CO;2-9, 1998.

Froidurot, S., Zin, I., Hingray, B., and Gautheron, A.: Sensitivity of Precipitation Phase over the Swiss Alps to Different Meteorological Variables, Journal of Hydrometeorology, 15, 685–696, https://doi.org/10.1175/JHM-D-13-073.1, 2014.

Gaál, L., Szolgay, J., Kohnová, S., Hlavčová, K., Parajka, J., Viglione, A., Merz, R., and Blöschl, G.: Dependence between flood peaks and volumes: a case study on climate and hydrological controls, Hydrological Sciences Journal, 60, 968–984, https://doi.org/10.1080/02626667.2014.951361, 2015.

Gafurov, A., Götzinger, J., and Bárdossy, A.: Hydrological modelling for meso-scale catchments using globally available data, https://doi.org/10.5194/hessd-3-2209-2006, 11 August 2006.

Gallice, A., Bavay, M., Brauchli, T., Comola, F., Lehning, M., and Huwald, H.: StreamFlow 1.0: an extension to the spatially distributed snow model Alpine3D for hydrological modelling and deterministic stream temperature prediction, Geosci. Model Dev., 9, 4491–4519, https://doi.org/10.5194/gmd-9-4491-2016, 2016.

Geris, J., Tetzlaff, D., Seibert, J., Vis, M., and Soulsby, C.: Conceptual Modelling to Assess Hydrological Impacts and Evaluate Environmental Flow Scenarios in Montane River Systems Regulated for Hydropower: MODELLING OF REGULATED MONTANE RIVERS, River Res. Applic., 31, 1066–1081, https://doi.org/10.1002/rra.2813, 2015.

Girons Lopez, M., Vis, M. J. P., Jenicek, M., Griessinger, N., and Seibert, J.: Assessing the degree of detail of temperature-based snow routines for runoff modelling in mountainous areas in central Europe, Hydrol. Earth Syst. Sci., 24, 4441–4461, https://doi.org/10.5194/hess-24-4441-2020, 2020a.

Girons Lopez, M., Vis, M. J. P., Jenicek, M., Griessinger, N., and Seibert, J.: Assessing the degree of detail of temperature-based snow routines for runoff modelling in mountainous areas in central Europe, Hydrol. Earth Syst. Sci., 24, 4441–4461, https://doi.org/10.5194/hess-24-4441-2020, 2020b.

Guan, H., Wilson, J. L., and Makhnin, O.: Geostatistical Mapping of Mountain Precipitation Incorporating Autosearched Effects of Terrain and Climatic Characteristics, Journal of Hydrometeorology, 6, 1018–1031, https://doi.org/10.1175/JHM448.1, 2005.

Hale, K. E., Musselman, K. N., Newman, A. J., Livneh, B., and Molotch, N. P.: Effects of Snow Water Storage on Hydrologic Partitioning Across the Mountainous, Western United States, Water Resources Research, 59, e2023WR034690, https://doi.org/10.1029/2023WR034690, 2023.

Harder, P. and Pomeroy, J.: Estimating precipitation phase using a psychrometric energy balance method, Hydrological Processes, 27, 1901–1914, https://doi.org/10.1002/hyp.9799, 2013.

Harpold, A. A. and Molotch, N. P.: Sensitivity of soil water availability to changing snowmelt timing in the western U.S., Geophysical Research Letters, 42, 8011–8020, https://doi.org/10.1002/2015GL065855, 2015.

He, B., Chang, J., Guo, A., Wang, L., Li, Z., Zhai, D., and Gao, F.: Spatial and temporal runoff variability in response to climate change in alpine mountains, Journal of Hydrology, 654, 132779, https://doi.org/10.1016/j.jhydrol.2025.132779, 2025.

https://doi.org/10.5194/egusphere-2026-2338
Preprint. Discussion started: 28 April 2026

Hegdahl, T. J., Engeland, K., Steinsland, I., and Singleton, A.: The benefits of pre- and postprocessing streamflow forecasts for an operational flood-forecasting system of 119 Norwegian catchments, https://doi.org/10.5194/hess-2021-13, 22 February 2021.

Hingray, B., Schaefli, B., Mezghani, A., and Hamdi, Y.: Signature-based model calibration for hydrological prediction in mesoscale Alpine catchments, Hydrological Sciences Journal, 55, 1002–1016, https://doi.org/10.1080/02626667.2010.505572, 2010.

Houze, R. A.: Orographic effects on precipitating clouds, Reviews of Geophysics, 50, 2011RG000365, https://doi.org/10.1029/2011RG000365, 2012.

Hublart, P. and Ruelland, D.: Reliability of lumped hydrological modeling in a semi-arid mountainous catchment facing water-use changes, Hydrol. Earth Syst. Sci., 2016.

Hunt, A. G., Sahimi, M., and Ghanbarian, B.: Predicting Streamflow Elasticity Based on Percolation Theory and Ecological Optimality, AGU Advances, 4, e2022AV000867, https://doi.org/10.1029/2022AV000867, 2023.

Immerzeel, W. W., Petersen, L., Ragettli, S., and Pellicciotti, F.: The importance of observed gradients of air temperature and precipitation for modeling runoff from a glacierized watershed in the Nepalese Himalayas, Water Resources Research, 50, 2212–2226, https://doi.org/10.1002/2013WR014506, 2014.

Isotta, F. A., Begert, M., and Frei, C.: Long-Term Consistent Monthly Temperature and Precipitation Grid Data Sets for Switzerland Over the Past 150 Years, JGR Atmospheres, 124, 3783–3799, https://doi.org/10.1029/2018JD029910, 2019.

Jenicek, M., Seibert, J., Zappa, M., Staudinger, M., and Jonas, T.: Importance of maximum snow accumulation for summer low flows in humid catchments, Hydrol. Earth Syst. Sci., 20, 859–874, https://doi.org/10.5194/hess-20-859-2016, 2016.

Jenicek, M., Seibert, J., and Staudinger, M.: Modeling of Future Changes in Seasonal Snowpack and Impacts on Summer Low Flows in Alpine Catchments, Water Resources Research, 54, 538–556, https://doi.org/10.1002/2017WR021648, 2018.

Jennings, K. S. and Molotch, N. P.: The sensitivity of modeled snow accumulation and melt to precipitation phase methods across a climatic gradient, Hydrol. Earth Syst. Sci., 23, 3765–3786, https://doi.org/10.5194/hess-23-3765-2019, 2019.

Jiang, Q.: Moist dynamics and orographic precipitation, Tellus A: Dynamic Meteorology and Oceanography, 55, 301, https://doi.org/10.3402/tellusa.v55i4.14577, 2003.

Knowles, N., Dettinger, M. D., and Cayan, D. R.: Trends in Snowfall versus Rainfall in the Western United States, Journal of Climate, 19, 4545–4559, https://doi.org/10.1175/JCLI3850.1, 2006.

Kobold, M. and Brilly, M.: The use of HBV model for flash flood forecasting, Nat. Hazards Earth Syst. Sci., 6, 407–417, https://doi.org/10.5194/nhess-6-407-2006, 2006.

Kritidou, E., Kauzlaric, M., Staudinger, M., Evin, G., Hingray, B., Vis, M., Seibert, J., and Viviroli, D.: Impact of different weather generator scenarios on extreme flood estimates in Switzerland, Stoch Environ Res Risk Assess, 39, 847–866, https://doi.org/10.1007/s00477-024-02843-8, 2025.

Kritidou, E., Kauzlaric, M., Staudinger, M., Evin, G., Hingray, B., Vis, M., and Viviroli, D.: Partitioning uncertainties of extreme flood estimates using long continuous simulations, Journal of Hydrology, 668, 134804, https://doi.org/10.1016/j.jhydrol.2025.134804, 2026.

https://doi.org/10.5194/egusphere-2026-2338
Preprint. Discussion started: 28 April 2026

Kumar, B., Roy, D., and Lakshmi, V.: Impact of temperature and precipitation lapse rate on hydrological modelling over Himalayan Gandak River Basin, J. Mt. Sci., 19, 3487–3502, https://doi.org/10.1007/s11629-020-6602-5, 2022.

Legrand, C., Hingray, B., Wilhelm, B., and Ménégoz, M.: Assessing downscaling methods to simulate hydrologically relevant weather scenarios from a global atmospheric reanalysis: case study of the upper Rhône River (1902–2009), Hydrol. Earth Syst. Sci., 28, 2139–2166, https://doi.org/10.5194/hess-28-2139-2024, 2024.

Lehning, M., Völksch, I., Gustafsson, D., Nguyen, T. A., Stähli, M., and Zappa, M.: ALPINE3D: a detailed model of mountain surface processes and its application to snow hydrology, Hydrological Processes, 20, 2111–2128, https://doi.org/10.1002/hyp.6204, 2006.

Luce, C. H., Lopez-Burgos, V., and Holden, Z.: Sensitivity of snowpack storage to precipitation and temperature using spatial and temporal analog models, Water Resources Research, 50, 9447–9462, https://doi.org/10.1002/2013WR014844, 2014.

Marra, F., Armon, M., Borga, M., and Morin, E.: Orographic Effect on Extreme Precipitation Statistics Peaks at Hourly Time Scales, Geophysical Research Letters, 48, e2020GL091498, https://doi.org/10.1029/2020GL091498, 2021.

Masson, D. and Frei, C.: Spatial analysis of precipitation in a high-mountain region: exploring methods with multi-scale topographic predictors and circulation types, Hydrol. Earth Syst. Sci., 18, 4543–4563, https://doi.org/10.5194/hess-18-4543-2014, 2014.

Medina, S. and Houze, R. A.: Air motions and precipitation growth in Alpine storms, Quart J Royal Meteoro Soc, 129, 345–371, https://doi.org/10.1256/qj.02.13, 2003.

Mizukami, N., Koren, V., Smith, M., Kingsmill, D., Zhang, Z., Cosgrove, B., and Cui, Z.: The Impact of Precipitation Type Discrimination on Hydrologic Simulation: Rain–Snow Partitioning Derived from HMT-West Radar-Detected Brightband Height versus Surface Temperature Data, Journal of Hydrometeorology, 14, 1139–1158, https://doi.org/10.1175/JHM-D-12-035.1, 2013.

Morán-Tejeda, E., López-Moreno, J. I., and Beniston, M.: The changing roles of temperature and precipitation on snowpack variability in Switzerland as a function of altitude, Geophysical Research Letters, 40, 2131–2136, https://doi.org/10.1002/grl.50463, 2013.

Mott, R., Scipión, D., Schneebeli, M., Dawes, N., Berne, A., and Lehning, M.: Orographic effects on snow deposition patterns in mountainous terrain, JGR Atmospheres, 119, 1419–1439, https://doi.org/10.1002/2013JD019880, 2014.

Muelchi, R., Rössler, O., Schwanbeck, J., Weingartner, R., and Martius, O.: River runoff in Switzerland in a changing climate – runoff regime changes and their time of emergence, Hydrol. Earth Syst. Sci., 25, 3071–3086, https://doi.org/10.5194/hess-25-3071-2021, 2021.

Napoli, A., Crespi, A., Ragone, F., Maugeri, M., and Pasquero, C.: Variability of orographic enhancement of precipitation in the Alpine region, Sci Rep, 9, 13352, https://doi.org/10.1038/s41598-019-49974-5, 2019.

Nash, J. E. and Sutcliffe, J. V.: River flow forecasting through conceptual models part I — A discussion of principles, Journal of Hydrology, 10, 282–290, https://doi.org/10.1016/0022-1694(70)90255-6, 1970.

Naveau, P., Huser, R., Ribereau, P., and Hannart, A.: Modeling jointly low, moderate, and heavy rainfall intensities without a threshold selection, Water Resources Research, 52, 2753–2769, https://doi.org/10.1002/2015WR018552, 2016.

https://doi.org/10.5194/egusphere-2026-2338
Preprint. Discussion started: 28 April 2026

Nicótina, L., Alessi Celegon, E., Rinaldo, A., and Marani, M.: On the impact of rainfall patterns on the hydrologic response, Water Resources Research, 44, 2007WR006654, https://doi.org/10.1029/2007WR006654, 2008.

Nie, S., Luo, Y., Wu, T., Shi, X., and Wang, Z.: A merging scheme for constructing daily precipitation analyses based on objective bias-correction and error estimation techniques, JGR Atmospheres, 120, 8671–8692, https://doi.org/10.1002/2015JD023347, 2015.

Oudin, L., Andréassian, V., Mathevet, T., Perrin, C., and Michel, C.: Dynamic averaging of rainfall-runoff model simulations from complementary model parameterizations, Water Resources Research, 42, 2005WR004636, https://doi.org/10.1029/2005WR004636, 2006.

Panziera, L., James, C. N., and Germann, U.: Mesoscale organization and structure of orographic precipitation producing flash floods in the Lago Maggiore region, Quart J Royal Meteoro Soc, 141, 224–248, https://doi.org/10.1002/qj.2351, 2015.

Parajka, J., Merz, R., and Bloschl, G.: A comparison of regionalisation methods for catchment model parameters, Hydrology and Earth System Sciences, 2005.

Pellet, C. and Hauck, C.: Monitoring soil moisture from middle to high elevation in Switzerland: Set-up and first results from the SOMOMOUNT network, https://doi.org/10.5194/hess-2016-474, 14 September 2016.

Pepin, N. C., Arnone, E., Gobiet, A., Haslinger, K., Kotlarski, S., Notarnicola, C., Palazzi, E., Seibert, P., Serafin, S., Schöner, W., Terzago, S., Thornton, J. M., Vuille, M., and Adler, C.: Climate Changes and Their Elevational Patterns in the Mountains of the World, Reviews of Geophysics, 60, e2020RG000730, https://doi.org/10.1029/2020RG000730, 2022.

Pohl, E., Gloaguen, R., Andermann, C., and Knoche, M.: Glacier melt buffers river runoff in the P amir M ountains, Water Resources Research, 53, 2467–2489, https://doi.org/10.1002/2016WR019431, 2017.

Pool, S., Viviroli, D., and Seibert, J.: Prediction of hydrographs and flow-duration curves in almost ungauged catchments: Which runoff measurements are most informative for model calibration?, Journal of Hydrology, 554, 613–622, https://doi.org/10.1016/j.jhydrol.2017.09.037, 2017.

Pool, S., Vis, M., and Seibert, J.: Evaluating model performance: towards a non-parametric variant of the Kling-Gupta efficiency, Hydrological Sciences Journal, 63, 1941–1953, https://doi.org/10.1080/02626667.2018.1552002, 2018.

Pool, S., Vis, M., and Seibert, J.: Regionalization for Ungauged Catchments — Lessons Learned From a Comparative Large-Sample Study, Water Resources Research, 57, e2021WR030437, https://doi.org/10.1029/2021WR030437, 2021.

Prein, A. F., Rasmussen, R. M., Ikeda, K., Liu, C., Clark, M. P., and Holland, G. J.: The future intensification of hourly precipitation extremes, Nature Clim Change, 7, 48–52, https://doi.org/10.1038/nclimate3168, 2017.

Quéno, L., Mott, R., Morin, P., Cluzet, B., Mazzotti, G., and Jonas, T.: Snow redistribution in an intermediate-complexity snow hydrology modelling framework, The Cryosphere, 18, 3533–3557, https://doi.org/10.5194/tc-18-3533-2024, 2024.

Ragettli, S. and Pellicciotti, F.: Calibration of a physically based, spatially distributed hydrological model in a glacierized basin: On the use of knowledge from glaciometeorological processes to constrain model parameters, Water Resources Research, 48, 2011WR010559, https://doi.org/10.1029/2011WR010559, 2012.

Ragettli, S., Cortés, G., McPhee, J., and Pellicciotti, F.: An evaluation of approaches for modelling hydrological processes in high-elevation, glacierized Andean watersheds, Hydrological Processes, 28, 5674–5695, https://doi.org/10.1002/hyp.10055, 2014.

https://doi.org/10.5194/egusphere-2026-2338
Preprint. Discussion started: 28 April 2026

Ren, W. W., Yang, T., Huang, C. S., Xu, C. Y., and Shao, Q. X.: Improving monthly streamflow prediction in alpine regions: integrating HBV model with Bayesian neural network, Stoch Environ Res Risk Assess, 32, 3381–3396, https://doi.org/10.1007/s00477-018-1553-x, 2018.

Roe, G. H.: OROGRAPHIC PRECIPITATION, Annu. Rev. Earth Planet. Sci., 33, 645–671, https://doi.org/10.1146/annurev.earth.33.092203.122541, 2005.

Ruelland, D.: Should altitudinal gradients of temperature and precipitation inputs be inferred from key parameters in snow-hydrological models?, Hydrol. Earth Syst. Sci., 24, 2609–2632, https://doi.org/10.5194/hess-24-2609-2020, 2020.

Sankarasubramanian, A., Vogel, R. M., and Limbrunner, J. F.: Climate elasticity of streamflow in the United States, Water Resources Research, 37, 1771–1781, https://doi.org/10.1029/2000WR900330, 2001.

Sarmadi, F., Huang, Y., Thompson, G., Siems, S. T., and Manton, M. J.: Simulations of orographic precipitation in the Snowy Mountains of Southeastern Australia, Atmospheric Research, 219, 183–199, https://doi.org/10.1016/j.atmosres.2019.01.002, 2019.

Schaefli, B., Rinaldo, A., and Botter, G.: Analytic probability distributions for snow-dominated streamflow, Water Resources Research, 49, 2701–2713, https://doi.org/10.1002/wrcr.20234, 2013.

Seibert, J.: Multi-criteria calibration of a conceptual runoff model using a genetic algorithm, Hydrology and Earth System Sciences, 4, 215–224, https://doi.org/10.5194/hess-4-215-2000, 2000.

Seibert, J. and Bergström, S.: A retrospective on hydrological catchment modelling based on half a century with the HBV model, Hydrology and Earth System Sciences, 26, 1371–1388, https://doi.org/10.5194/hess-26-1371-2022, 2022.

Seibert, J. and Vis, M. J. P.: Teaching hydrological modeling with a user-friendly catchment-runoff-model software package, Hydrol. Earth Syst. Sci., 16, 3315–3325, https://doi.org/10.5194/hess-16-3315-2012, 2012.

Sevruk, B.: Regional Dependency of Precipitation-Altitude Relationship in the Swiss Alps, in: Climatic Change at High Elevation Sites, edited by: Diaz, H. F., Beniston, M., and Bradley, R. S., Springer Netherlands, Dordrecht, 123–137, https://doi.org/10.1007/978-94-015-8905-5_7, 1997.

Shahgedanova, M., Adler, C., Gebrekirstos, A., Grau, H. R., Huggel, C., Marchant, R., Pepin, N., Vanacker, V., Viviroli, D., and Vuille, M.: Mountain Observatories: Status and Prospects for Enhancing and Connecting a Global Community, Mountain Research and Development, 41, https://doi.org/10.1659/MRD-JOURNAL-D-20-00054.1, 2021.

Sikorska-Senoner, A. E., Schaefli, B., and Seibert, J.: Downsizing parameter ensembles for simulations of rare floods, Nat. Hazards Earth Syst. Sci., 20, 3521–3549, https://doi.org/10.5194/nhess-20-3521-2020, 2020.

Singh, B., Liu, M., Abatzoglou, J., Adam, J., and Rajagopalan, K.: Dynamic precipitation phase partitioning improves modeled simulations of snow across the Northwest US, https://doi.org/10.5194/egusphere-2024-2284, 16 August 2024.

Somers, L. D. and McKenzie, J. M.: A review of groundwater in high mountain environments, WIREs Water, 7, e1475, https://doi.org/10.1002/wat2.1475, 2020.

Sospedra-Alfonso, R., Melton, J. R., and Merryfield, W. J.: Effects of temperature and precipitation on snowpack variability in the Central Rocky Mountains as a function of elevation, Geophysical Research Letters, 42, 4429–4438, https://doi.org/10.1002/2015GL063898, 2015.

https://doi.org/10.5194/egusphere-2026-2338
Preprint. Discussion started: 28 April 2026

Staudinger, M., Stoelzle, M., Seeger, S., Seibert, J., Weiler, M., and Stahl, K.: Catchment water storage variation with elevation, Hydrological Processes, 31, 2000–2015, https://doi.org/10.1002/hyp.11158, 2017.

Staudinger, M., Kauzlaric, M., Mas, A., Evin, G., Hingray, B., and Viviroli, D.: The role of antecedent conditions in translating precipitation events into extreme floods at the catchment scale and in a large-basin context, Nat. Hazards Earth Syst. Sci., 25, 247–265, https://doi.org/10.5194/nhess-25-247-2025, 2025.

Stephens, T. A. and Bledsoe, B. P.: Flood Protection Reliability: The Impact of Uncertainty and Nonstationarity, Water Resources Research, 59, e2021WR031921, https://doi.org/10.1029/2021WR031921, 2023.

Suri, A. and Azad, S.: Optimal placement of rain gauge networks in complex terrains for monitoring extreme rainfall events: a review, Theor Appl Climatol, 155, 2511–2521, https://doi.org/10.1007/s00704-024-04856-3, 2024.

Tang, Y., Tang, Q., Wang, Z., Chiew, F. H. S., Zhang, X., and Xiao, H.: Different Precipitation Elasticity of Runoff for Precipitation Increase and Decrease at Watershed Scale, JGR Atmospheres, 124, 11932–11943, https://doi.org/10.1029/2018JD030129, 2019.

Turpin, O. C., Caves, R. G., Ferguson, R. I., and Johansson, B.: Verification of simulated snow cover in an Arctic basin using satellite-derived snow-cover maps, Ann. Glaciol., 31, 391–396, https://doi.org/10.3189/172756400781819932, 2000.

Verbunt, M., Gurtz, J., Jasper, K., Lang, H., Warmerdam, P., and Zappa, M.: The hydrological role of snow and glaciers in alpine river basins and their distributed modeling, Journal of Hydrology, 282, 36–55, https://doi.org/10.1016/S0022-1694(03)00251-8, 2003.

Vergara-Temprado, J., Ban, N., and Schär, C.: Extreme Sub-Hourly Precipitation Intensities Scale Close to the Clausius-Clapeyron Rate Over Europe, Geophysical Research Letters, 48, e2020GL089506, https://doi.org/10.1029/2020GL089506, 2021.

Viviroli, D., Dürr, H. H., Messerli, B., Meybeck, M., and Weingartner, R.: Mountains of the world, water towers for humanity: Typology, mapping, and global significance, Water Resources Research, 43, 2006WR005653, https://doi.org/10.1029/2006WR005653, 2007.

Viviroli, D., Archer, D. R., Buytaert, W., Fowler, H. J., Greenwood, G. B., Hamlet, A. F., Huang, Y., Koboltschnig, G., Litaor, M. I., López-Moreno, J. I., Lorentz, S., Schädler, B., Schreier, H., Schwaiger, K., Vuille, M., and Woods, R.: Climate change and mountain water resources: overview and recommendations for research, management and policy, Hydrol. Earth Syst. Sci., 15, 471–504, https://doi.org/10.5194/hess-15-471-2011, 2011.

Viviroli, D., Sikorska-Senoner, A. E., Evin, G., Staudinger, M., Kauzlaric, M., Chardon, J., Favre, A.-C., Hingray, B., Nicolet, G., Raynaud, D., Seibert, J., Weingartner, R., and Whealton, C.: Comprehensive space–time hydrometeorological simulations for estimating very rare floods at multiple sites in a large river basin, Nat. Hazards Earth Syst. Sci., 22, 2891–2920, https://doi.org/10.5194/nhess-22-2891-2022, 2022.

Wasko, C. and Guo, D.: Understanding event runoff coefficient variability across Australia using the *HYDROEVENTS R* package, Hydrological Processes, 36, e14563, https://doi.org/10.1002/hyp.14563, 2022.

Wasko, C. and Nathan, R.: Influence of changes in rainfall and soil moisture on trends in flooding, Journal of Hydrology, 575, 432–441, https://doi.org/10.1016/j.jhydrol.2019.05.054, 2019.

Weiler, M., Gnann, S., and Stahl, K.: Streamflow sensitivity regimes of alpine catchments: seasonal relationships with elevation, temperature, and glacier cover, Environ. Res. Lett., 20, 074068, https://doi.org/10.1088/1748-9326/ade26c, 2025.

https://doi.org/10.5194/egusphere-2026-2338
Preprint. Discussion started: 28 April 2026

Wilks, D. S.: Multisite generalization of a daily stochastic precipitation generation model, Journal of Hydrology, 210, 178–191, https://doi.org/10.1016/S0022-1694(98)00186-3, 1998.

Wortmann, M., Bolch, T., Menz, C., Tong, J., and Krysanova, V.: Comparison and Correction of High-Mountain Precipitation Data Based on Glacio-Hydrological Modeling in the Tarim River Headwaters (High Asia), Journal of Hydrometeorology, 19, 777–801, https://doi.org/10.1175/JHM-D-17-0106.1, 2018.

Zelelew, M. B. and Alfredsen, K.: Sensitivity-guided evaluation of the HBV hydrological model parameterization, Journal of Hydroinformatics, 15, 967–990, https://doi.org/10.2166/hydro.2012.011, 2013.

Zhang, F., Zhang, H., Hagen, S. C., Ye, M., Wang, D., Gui, D., Zeng, C., Tian, L., and Liu, J.: Snow cover and runoff modelling in a high mountain catchment with scarce data: effects of temperature and precipitation parameters: SNOW-HYDROLOGICAL MODELLING IN A HIGH MOUNTAIN CATCHMENT, Hydrol. Process., 29, 52–65, https://doi.org/10.1002/hyp.10125, 2015.

Zhang, Y., Viglione, A., and Blöschl, G.: Temporal Scaling of Streamflow Elasticity to Precipitation: A Global Analysis, Water Resources Research, 58, e2021WR030601, https://doi.org/10.1029/2021WR030601, 2022.

Zhou, S., Wang, Y., Li, Z., Chang, J., and Guo, A.: Quantifying the Uncertainty Interaction Between the Model Input and Structure on Hydrological Processes, Water Resour Manage, 35, 3915–3935, https://doi.org/10.1007/s11269-021-02883-7, 2021a.

Zhou, X., Ma, W., Echizenya, W., and Yamazaki, D.: The uncertainty of flood frequency analyses in hydrodynamic model simulations, Nat. Hazards Earth Syst. Sci., 21, 1071–1085, https://doi.org/10.5194/nhess-21-1071-2021, 2021b.